PLANT SCIENCES

Arabidopsis TIE1 and TIE2 transcriptional repressors dampen cytokinin response during root development

Qing He†, Rongrong Yuan†, Tiantian Zhang, Fengying An, Ning Wang, Jingqiu Lan, Xinxue Wang, Zeliang Zhang, Yige Pan, Xuanzhi Wang, Jinzhe Zhang, Dongshu Guo, Genji Qin*

Cytokinin plays critical roles in root development. Cytokinin signaling depends on activation of key transcription factors known as type B *Arabidopsis* response regulators (ARRs). However, the mechanisms underlying the finely tuned regulation of type B ARR activity remain unclear. In this study, we demonstrate that the ERF-associated amphiphilic repression (EAR) motif–containing protein TCP interactor containing ear motif protein2 (TIE2) forms a negative feedback loop to finely tune the activity of type B ARRs during root development. Disruption of *TIE2* and its close homolog TIE1 causes severely shortened roots. TIE2 interacts with type B ARR1 and represses transcription of ARR1 targets. The cytokinin response is correspondingly enhanced in *tie1-1 tie2-1*. We further show that ARR1 positively regulates *TIE1* and *TIE2* by directly binding to their promoters. Our findings demonstrate that TIEs play key roles in controlling plant development and reveal an important negative feedback regulation mechanism for cytokinin signaling.

INTRODUCTION

The plant root system is essential for plant survival because of its critical role in absorption of nutrients and water from the soil and provision of anchorage. Thus, the developmental plasticity of roots is essential for adaptation of sessile plants to diverse soil conditions (*1*). In *Arabidopsis*, the mature root is longitudinally divided into the stem cell niche (SCN), the proliferation zone (PZ), the transition zone (TZ), the elongation zone (EZ), and the differentiation zone (DZ) (*2*). When the roots grow, the stem cells surrounding the quiescent center (QC) in the SCN asymmetrically divide to generate stem cell daughters. The daughter cells further divide several times in the PZ and then transit to the EZ via the TZ. Cells in the EZ elongate longitudinally and enter the DZ for differentiation (*2*). The plasticity of root growth and development is determined by coordinated cell division, elongation, and differentiation in the PZ, TZ, EZ, and DZ, which are tightly regulated by various internal hormones and external conditions (*2*).

The phytohormone cytokinin is one of the most important hormones governing root development (*3*). Genetic and mutant analysis indicates that cytokinin negatively regulates the size of the root meristem by repressing cell division in the PZ and promoting cell differentiation in the TZ (*4*–*6*). Disruption of genes in cytokinin biosynthesis or signaling leads to a larger root meristem (*4*). In the EZ, cytokinin inhibits cell elongation by altering the direction of microtubule disposition (*7*). Cytokinin applications result in shorter roots (*8*), while the disruption of type B *Arabidopsis* response regulators (ARRs), which play key roles in cytokinin signaling, produces longer roots in *arr1*, *arr1 arr12*, and *arr1 arr10 arr12* mutants (*9*, *10*). In the DZ, cytokinin positively regulates root hair development. Application of cytokinin increases the density of root hairs (*11*). In addition, cytokinin represses the emergence of lateral roots and responses to environmental conditions (*8*, *9*). These findings suggest that cytokinin regulates root morphology by participating in almost all aspects of root development, and thus, tight regulation of cytokinin signal output is pivotal for root developmental plasticity.

State Key Laboratory of Protein and Plant Gene Research, School of Life Sciences, Peking University, Beijing 100871, People's Republic of China.
*Corresponding author. Email: qingenji@pku.edu.cn
†These authors contributed equally to this work.

Cytokinin is perceived by a group of *Arabidopsis* histidine kinase (AHK) receptors and triggers a multistep phosphorelay, in which AHKs are first autophosphorylated and the phosphate is lastly relayed to a class of ARR transcription factors via *Arabidopsis* histidine protein 1 to 5 (AHP1 to AHP5) to elicit the cytokinin response (*12*, *13*). Eleven type B, 10 type A, and 2 type C ARRs comprise the *Arabidopsis* ARR family. The type B ARRs contain an N-terminal receiver domain and a C-terminal MYB-like DNA binding domain, whereas type A ARRs lack a DNA binding domain (*12*, *13*). Phosphorylation of a conserved aspartate (Asp) in the receiver domain by cytokinin leads to the activation of type B ARRs (*14*). Type B ARRs mediate major cytokinin-dependent transcriptional outputs and directly regulate thousands of genes (*15*–*17*). Tight regulation of the activity of type B ARRs is very important for fine-tuning of the cytokinin response at appropriate spatiotemporal scales and, thus, for plant developmental plasticity (*15*–*17*). To accurately tune cytokinin outputs, some genes, including cytokinin oxidases (*CKX*), *AHK4*, *AHP6*, and type A *ARRs* are up-regulated by cytokinin and, in turn, dampen cytokinin signaling in negative feedback loops (*13*). CKXs decrease the level of cytokinin by mediating cytokinin degradation (*13*). AHK4 acts as a phosphatase and dephosphorylates AHPs in the absence of cytokinin (*18*). AHP6 has no conserved phosphorylation site and competes with other AHPs for interaction with AHK receptors, while type A ARRs may compete with type B ARRs for the phosphate transferred by AHPs (*19*). In addition, KISS ME DEADLY (*KMD*) family genes encoding F-box proteins negatively regulate the cytokinin response by forming S-phase kinase-associated protein1/Cullin/F-box protein E3 ubiquitin ligase complexes to mediate several type B ARR proteins for degradation via the 26*S* proteasome (*20*). However, the molecular mechanisms by which plants finely control cytokinin outputs in various developmental contexts remain to be elucidated.

The ethylene response factor (ERF)–associated amphiphilic repression (EAR) motif has been identified as a plant-specific repression domain with a conserved short sequence LXLXL (L indicates leucine, and X represents any amino acid) (*21*). More than 200 transcriptional regulators in the *Arabidopsis* genome have been found to contain the EAR motif (*22*). Many of them have been identified to be essential for different biological processes (*22*). For

example, EAR motif–containing proteins are repeatedly used by plants to control hormone signaling pathways. Auxin/indole-3-acetic acid (AUX/IAA), novel interactor of jaz (NINJA), suppressor of more axillary growth2 1-like (SMXL), ABI five binding protein (AFP), and brassinazole-resistant 1 (BZR1) proteins are well-known EAR motif–containing transcriptional repressors that play pivotal roles in the auxin (*23*), jasmonic acid (JA) (*24*), strigolactone (SL) (*25*), abscisic acid (ABA) (*24*), and brassinosteroid (BR) pathways (*26*), respectively. It has been proposed that these different EAR motif–containing proteins recruit topless/topless-related (TPL/TPR) co-repressors and histone deacetylases (HDAs) to cause local chromatin condensation and, thus, the repression of key transcription factors in hormone signaling pathways (*27*). Although cytokinin causes dynamic changes in chromatin condensation for which type B ARRs are necessary (*28*), no EAR motif–containing transcriptional repressors have yet been found to regulate the activity of type B ARR transcription factors in the cytokinin signaling pathway.

We previously identified TCP interactor containing EAR motif protein 1 (TIE1) by analyzing a T-DNA activation tagging curly leaf mutant *tie1-D* (*29*). TIE1 contains a C-terminal EAR motif that recruits TPL/TPRs to repress the activity of teosinte branched1/cycloidea/proliferating cell factor (TCP) family transcription factors during leaf development and shoot branching (*29*, *30*). We further demonstrated that TIE1 is regulated by degradation via the 26*S* proteasome, and we showed that the degradation of TIE1 is mediated by TIE1-associated ring-type E3 ligase1 (TEAR1) (*31*). TIE1 has three close homologs in the *Arabidopsis* genome: TIE2, TIE3, and TIE4. They all contain EAR motifs at the C terminus and interact with TPL/TPR co-repressors (*29*). Overexpression of *TIE2*, *TIE3*, or *TIE4* causes curly leaves resembling those observed in *TIE1* overexpression mutant *tie1-D* (*29*), suggesting that these four proteins may have similar biochemical functions. Among these four *TIE*s, *TIE2* is predominantly expressed in roots (*29*). However, the roles of TIE2 and other TIEs during root development are still unknown.

In this study, we generated a *tie1-1 tie2-1* double mutant and observed that *tie1-1 tie2-1* produced obviously shorter roots, indicating that TIE1 and TIE2 play an important role in root elongation. *TIE1* and *TIE2* are predominantly expressed in the EZ and DZ and specifically control the length of cells in the EZ and DZ. We show that the N terminus of TIE2 interacts with several type B ARR transcription factors, including ARR1 and ARR2, and the C-terminal EAR motif is required for its repression activity. The expression of an ARR1 or ARR2 fusion protein with the C terminus of TIE2 rescues the shorter roots of *tie1-1 tie2-1*. We further demonstrate that ARR1 directly up-regulates *TIE1* and *TIE2* by binding to their promoter regions. Therefore, our findings elucidate the important roles of TIE1 and TIE2 in the control of root developmental plasticity and establish an unknown negative feedback loop in cytokinin signaling during root development. In this loop, cytokinin activates type B ARRs to directly promote transcription of *TIE1* and *TIE2*, and the increased abundance of TIE1 and TIE2, in turn, suppresses cytokinin signaling by inhibiting the activity of type B ARRs.

RESULTS

The double mutant *tie1-1 tie2-1* produced short roots

TIE2 is a homolog of TIE1 that acts as a transcriptional repressor. In comparison with *TIE1*, which is expressed in both roots and shoots, *TIE2* is predominantly expressed in roots (*29*). To reveal the possible roles of TIE2 in root development, we first generated a *tie2-1* mutant with a 7–base pair (bp) deletion in the first exon of the *TIE2* gene using CRISPR-Cas9 technology (fig. S1B). The roots of *tie2-1* had no obvious phenotype when compared to those of wild-type plants (fig. S1, D and E). To overcome potential functional redundancy, we identified a new *tie1-1* (*GABI_372F04*) mutant, in which T-DNA was inserted into the first exon of *TIE1* (fig. S1A). The T-DNA insert disrupted the function of *TIE1* in *tie1-1* (fig. S1C). The *tie1-1* mutant also displayed roots that were comparable to those of the wild-type control (fig. S1, D and E). Next, we crossed *tie2-1* and *tie1-1* to generate the *tie1-1 tie2-1* double mutant. We observed that *tie1-1 tie2-1* displayed severely shorter roots and produced obviously fewer lateral roots (Fig. 1, A to D). To confirm that the root defects in *tie1-1 tie2-1* were caused by disruption of *TIE1* or *TIE2*, we generated TIE1pro-TIE1-GFP (green fluorescent protein) and TIE2pro-TIE2-GFP constructs, in which the sequence encoding GFP at the C-terminal end of TIE1 or TIE2 was driven by their own promoters, respectively. Either TIE1pro-TIE1-GFP or TIE2pro-TIE2-GFP transformation completely rescued the shorter roots of *tie1-1 tie2-1* (Fig. 1E and fig. S2). We next investigate the root length of an activation tagging mutant *tie1-D* in which *TIE1* gene is overexpressed (*29*). The results showed that *tie1-D* produced longer roots and exhibited a root phenotype opposite to *tie1-1 tie2-1* (fig. S3, A to D). These results indicate that TIEs play key roles in root elongation.

To comprehensively assess the root phenotypes of *tie1-1 tie2-1*, we first performed starch staining with Lugol's solution (*32*), which showed that the distribution of starch granules and the columella cell differentiation in the roots of *tie1-1 tie2-1* had no obvious differences from that of wild-type plants (fig. S4, A and B). We then introduced the QC marker WUSCHEL-related homeobox 5 (WOX5)::GFP into *tie1-1 tie2-1* (fig. S4, C and D) (*33*). GFP fluorescence was clearly observed in the QC of *tie1-1 tie2-1* and wild-type controls. These results indicate that the QC identity and the columella cell differentiation have no obvious defects in the roots of *tie1-1 tie2-1*. We next investigated the size of the root meristem, as indicated by the number of cells in a cortex file from the QC to the first elongated cell. The statistical analysis showed that the size of the root meristem in the roots of *tie1-1 tie2-1* was also not substantially different from that of the wild-type controls (Fig. 1, F, G, and I). We confirmed that the root meristem was not affected by disruption of *TIE1* and *TIE2* in *tie1-1 tie2-1* by introducing Cyclin B1;1:GUS (β-glucuronidase) into *tie1-1 tie2-1* and GUS staining analysis (Fig. 1, J to L). We then observed the cells in the EZ and DZ of *tie1-1 tie2-1*. The results showed that cell elongation in the EZ and DZ was severely affected in *tie1-1 tie2-1* (Fig. 1, H and M), and the cells were significantly shorter than those of the wild-type control (Fig. 1M). These results indicate that TIE1 and TIE2 control root length by promoting cell elongation in the EZ and thus increasing the cell length in the DZ.

TIE1 and *TIE2* have overlapping expression in the EZ and DZ

To elucidate the spatiotemporal expression pattern of *TIE1* and *TIE2* during root development, we generated TIE1pro-GUS and TIE2pro-GUS constructs, in which the *GUS* gene was driven by a 2790-bp-long *TIE1* promoter or a 5104-bp-long *TIE2* promoter. The roots of more than 30 independent TIE1pro-GUS or TIE2pro-GUS transgenic lines displayed similar expression patterns. We subjected one stable TIE1pro-GUS line and one stable TIE2pro-GUS line to detailed analysis. In 1-day-old germinated seeds, *TIE1* was found to

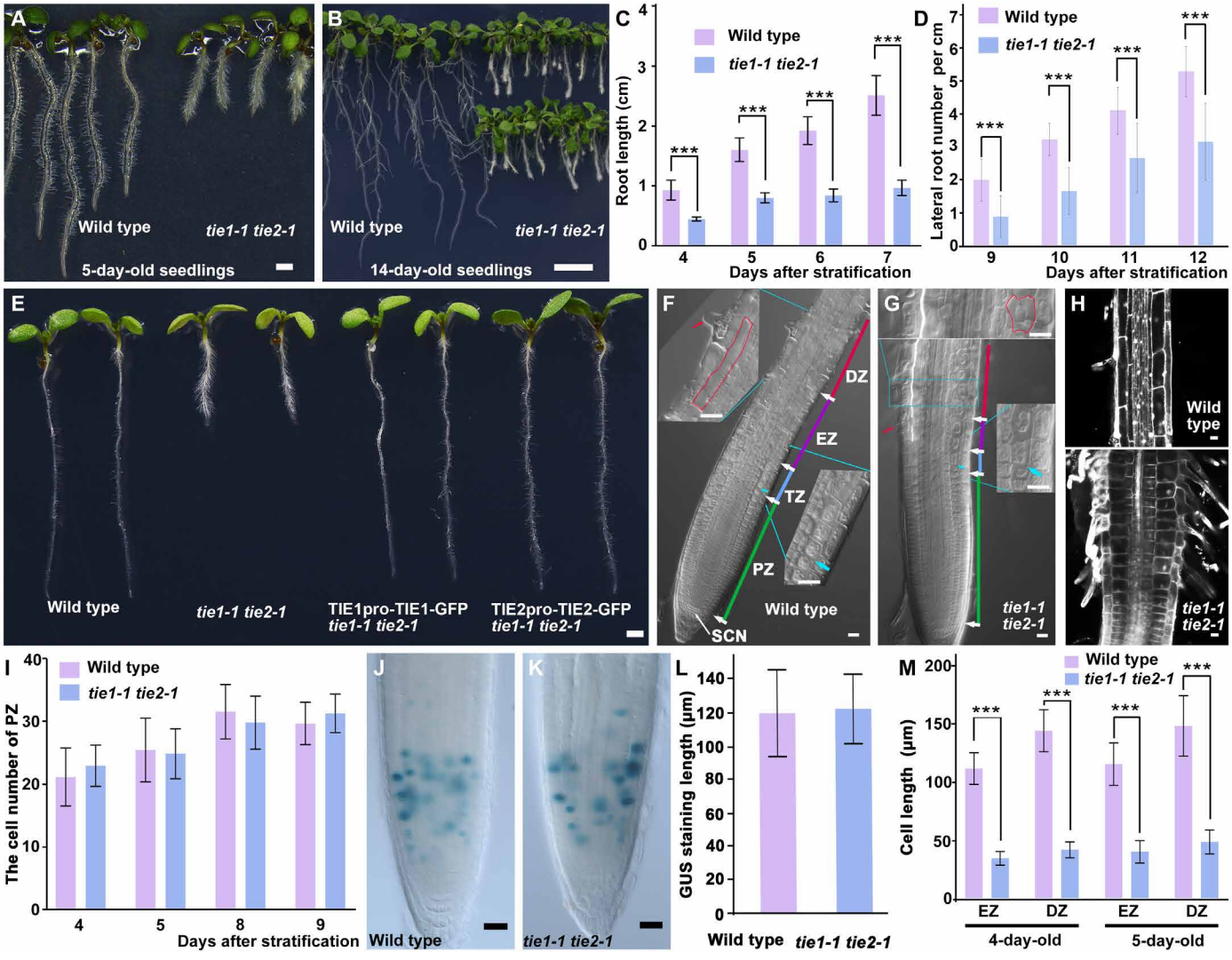

Fig. 1. The *tie1-1 tie2-1* double mutant displayed severely shorter roots and fewer lateral roots. (**A**) Five-day-old wild type and *tie1-1 tie2-1*. (**B**) Fourteen-day-old wild type and *tie1-1 tie2-1*. (**C**) The length of roots from wild type and *tie1-1 tie2-1*. Data are means ± SD ($n = 21$) of three independent experiments. (**D**) The density of lateral roots from wild type and *tie1-1 tie2-1*. Data are means ± SD ($n = 34$ for wild type and $n = 67$ for *tie1-1 tie2-1*) of three independent experiments. (**E**) Complementation of *tie1-1 tie2-1* by transforming TIE1pro-TIE1-GFP or TIE2pro-TIE2-GFP. (**F** and **G**) Observation of the root meristem, EZ, and DZ of the longitudinal roots from wild type and *tie1-1 tie2-1*. (**H**) Propidium iodide (PI) staining of roots shows the elongation of cells in the EZ and the DZ of roots from wild type (top) and *tie1-1 tie2-1* (bottom). (**I**) The cell number of the root meristems from wild type and *tie1-1 tie2-1*. Data are means ± SD ($n = 17$) of three independent experiments. (**J** and **K**) CyclinB1;1:GUS staining of the root meristem in the wild-type or *tie1-1 tie2-1* background. (**L**) Statistical analysis of the length of GUS staining regions in the wild-type or *tie1-1 tie2-1* roots shown in (J and K). Data are means ± SD ($n = 22$) of three independent experiments. (**M**) The length of cells in the EZ and DZ of roots from 4- and 5-day-old wild type and *tie1-1 tie2-1*. Data are means ± SD ($n = 38$) of three independent experiments. Scale bar, 1 mm (A, B, and E) and 25 μm (F to H, J, and K). Student's *t* test was used for significance testing, ***$P < 0.001$ in (C, D, I, L, and M).

be expressed in the cotyledons, while no expression of *TIE1* was observed in the protruded root tips (Fig. 2A). *TIE1* started to be expressed in the proximal part of the root, but not in the root tip, of 1.5-day-old TIE1pro-GUS plants (Fig. 2B). The expression pattern was maintained as plants grew, with no expression in the root tip (Fig. 2, C to G). Strong GUS staining was found in the roots, excluding the root tips, in the 2-, 3-, 4-, 5-, and 9-day-old TIE1pro-GUS seedlings (Fig. 2, C to G). GUS staining was also observed at the initial sites of lateral roots (Fig. 2G). The young lateral roots had a similar expression pattern, with GUS staining in the proximal parts but not in the lateral root tips (Fig. 2G). The expression pattern shown by TIE1pro-GUS in the vasculature and root tip is consistent with the results that we reported previously (*29*). In comparison with *TIE1*, no GUS staining was observed in the root of 1-day-old germinated seed from TIE2pro-GUS plant (Fig. 2H). *TIE2* was clearly expressed in the roots of the 2-, 3-, 4-, 5-, and 9-day-old seedlings (Fig. 2, I to M). A small region neighboring the root tip never showed GUS staining in the roots (Fig. 2, I to M). As the plants grew, the GUS staining faded in the root region near the hypocotyl (Fig. 2, J to M). The expression of *TIE2* was also found at the initial sites of lateral roots (Fig. 2M). The expression pattern of the young lateral roots was like that of the main roots (Fig. 2M). To further

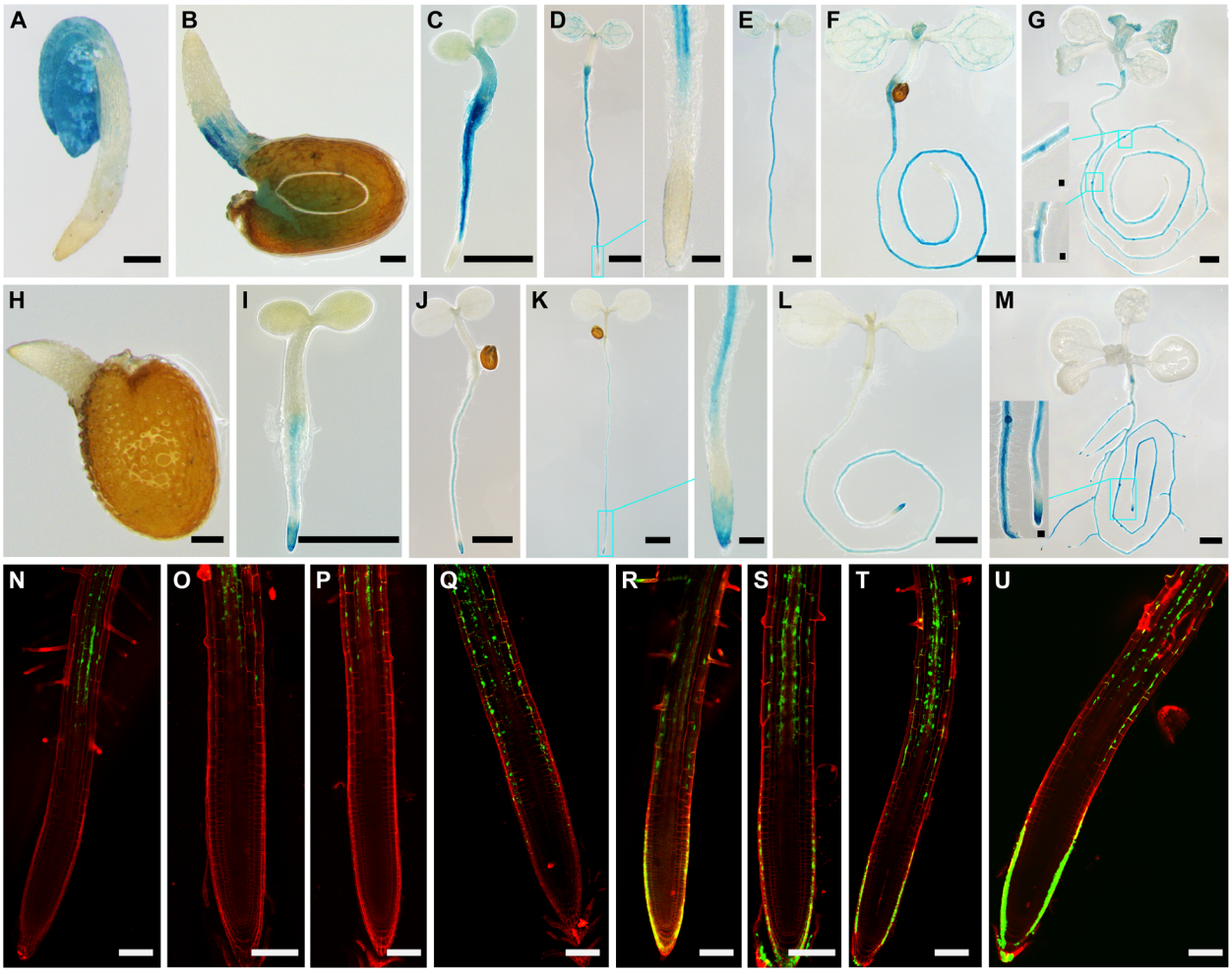

Fig. 2. The expression patterns of *TIE1* and *TIE2* in the roots. (**A** to **G**) GUS staining of the stable *TIE1pro-GUS* transgenic line. (A) A 1-day-old seedling. (B) A 1.5-day-old seedling. (C) A 2-day-old seedling. (D) A 3-day-old seedling. (E) A 4-day-old seedling. (F) A 5-day-old seedling. (G) A 9-day-old seedling. The close-up view in (D) shows staining of the root tip. The close-up view in (G) shows GUS staining in the lateral roots. (**H** to **M**) GUS staining of the stable *TIE2pro-GUS* transgenic line. (H) A 1-day-old seedling. (I) A 2-day-old seedling. (J) A 3-day-old seedling. (K) A 4-day-old seedling. (L) A 5-day-old seedling. (M) A 9-day-old seedling. The close-up view in (K) shows staining of the root tip. The close-up view in (M) shows GUS staining in the lateral roots. (N to Q) GFP fluorescence of 3-, 4-, 5-, and 7-day-old TIE1pro-TIE1-GFP roots. (**R** to **U**) GFP fluorescence of 3-, 4-, 5-, and 7-day-old TIE2pro-TIE2-GFP roots. Scale bars, 0.1 mm [(A, B, H, and N to U) and insets of (D, G, K, and M)] and 1 mm (C to G and I to M).

determine the expression patterns of *TIE1* and *TIE2* in the root tip region, we observed the GFP fluorescence of TIE1pro-TIE1-GFP and TIE2pro-TIE2-GFP, which complemented the shorter root phenotype of *tie1-1 tie2-1*. Clear GFP fluorescence was observed in the TZ and DZ, but not in the root meristem, in TIE1pro-TIE1-GFP roots (Fig. 2, N to Q). In TIE2pro-TIE2-GFP roots, GFP fluorescence was found in the TZ, the DZ, columella cells, and lateral root cap (Fig. 2, R to U). These results suggest that both *TIE1* and *TIE2* are expressed in specific root domains, and the expression patterns of *TIE1* and *TIE2* overlap in the EZ and DZ, corresponding to the shorter cells in the EZ and DZ in the roots of *tie1-1 tie2-1*.

TIE2 is a transcriptional repressor

TIE1 was previously demonstrated to be a transcriptional repressor. Overexpression of *TIE2* leads to curly leaves resembling those of *TIE1* activation tagging mutant *tie1-D*, suggesting that *TIE2* may also encode a transcriptional repressor (*29*). To confirm that TIE2 can function as a transcriptional repressor in nuclei, we first observed the fluorescence of TIE2pro-TIE2-GFP, which rescued the shorter root phenotype of *tie1-1 tie2-1*. The GFP fluorescence of TIE2-GFP was distributed in the cytoplasm and nuclei, but the signals were clearer and stronger in nuclei (Fig. 3, A to C, and fig. S5). We next generated the reporter 35S-UAS-LUC, in which the *Luciferase* (*LUC*) gene was driven by a synthetic promoter containing a cauliflower mosaic virus (CaMV) 35S promoter fusion with six upstream activating sequences (UAS) bound by GAL4, and the reporter 35S-REN-35S-UAS-LUC, in which the *Renilla Luciferase* (*REN*) gene was driven by a CaMV 35S promoter, and used it as an internal expression control (Fig. 3D). We generated the effector 35S-G4BD-TIE2 in which a CaMV 35S promoter was used to drive *TIE2* fusion to the sequence encoding the GAL4 DNA binding domain (G4BD). We also generated the control vector 35S-G4BD or 35S-G4BD-TIE2mEAR in which a CaMV 35S promoter was used to drive *G4BD* or *G4BD*

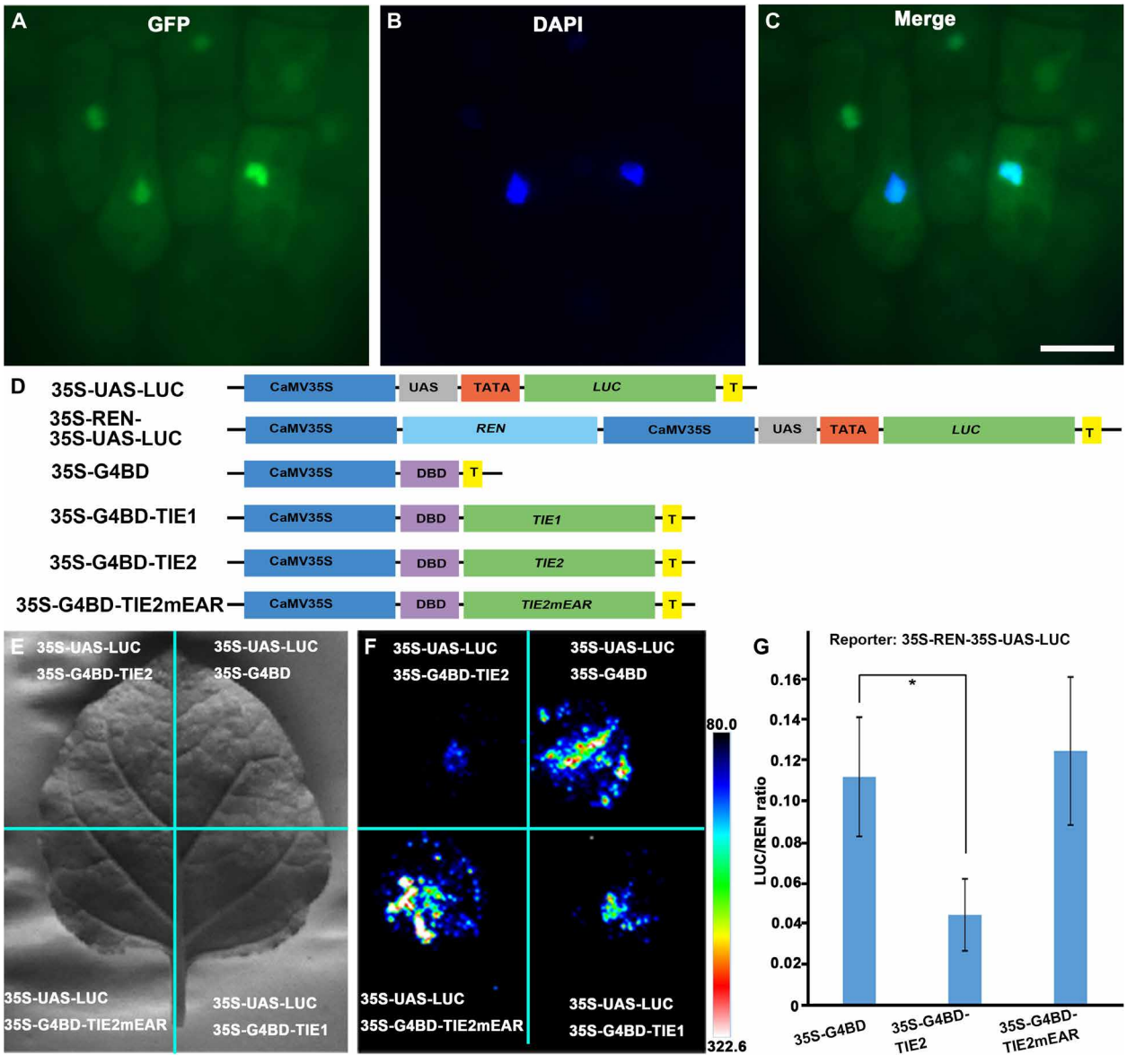

Fig. 3. TIE2 is a nuclear transcriptional repressor. (**A** to **C**) The subcellular localization of TIE2 is shown by the GFP fluorescence in the cells of roots from TIE2pro-TIE2-GFP plants, which rescued the short root phenotype of *tie1-1 tie2-1*. TIE2 was predominantly localized to nuclei. (A) GFP fluorescence. (B) DAPI (4′,6-diamidino-2-phenylindole) staining. (C) The merged picture of (A) and (B). Scale bar, 10 μm. (**D**) A schematic representation of the constructs used in (E to G). (E and F) TIE2 displayed transcriptional repression activity similar to that of TIE1, and the EAR motif was required for the repression activity. (**E**) Bright-field image and (**F**) fluorescence of tobacco leaves cotransformed with the different combinations of constructs shown in (D). (**G**) The protoplast transient expression system indicated that TIE2 acts as a transcriptional repressor. 35S-REN-35S-UAS-LUC was transformed into *Arabidopsis* protoplasts with 35S-G4BD, 35S-G4BD-TIE2, or 35S-G4BD-TIE2mEAR, respectively, and the LUC/REN ratio was measured. The data are means (± SD) of three replicates. Student's *t* test was used for significance testing, $^*P < 0.05$.

fusion with *TIE2mEAR* encoding mutated TIE2 with the three mutations (the conserved L was mutated to S) in the EAR motif. We cotransformed 35S-UAS-LUC with 35S-G4BD-TIE2, the negative control 35S-G4BD, 35S-G4BD-TIE2mEAR, or the positive control 35S-G4BD-TIE1 into tobacco leaves (Fig. 3, E and F). The results showed that *LUC* reporter expression was higher in leaves transformed with the combination with 35S-G4BD, as shown by the stronger fluorescence, while the expression of *LUC* was repressed in the leaves transformed with the combination with 35S-G4BD-TIE2 or 35S-G4BD-TIE1, suggesting that TIE2 and TIE1 had transcriptional repression activity. However, repression of the *LUC* reporter was released by transforming with the combination with 35S-G4BD-TIE2mEAR, indicating that the EAR motif was required for the repression activity of TIE2 (Fig. 3, E and F). We then cotransformed the 35S-REN-35S-UAS-LUC reporter with 35S-G4BD, 35S-G4BD-TIE2, or 35S-G4BD-TIE2mEAR into *Arabidopsis* protoplasts. The quantitative analysis showed that TIE2 repressed the reporter *LUC*, and the EAR motif was required for the repression (Fig. 3G). These results indicate that TIE2 is an EAR motif–containing regulator with transcriptional repression activity.

TIE2 interacts with type B ARR1 to repress its transactivation activity

We previously screened an *Arabidopsis* transcription factor library using the N terminus of TIE1 as bait (*29*). We found that type B ARR11 and some other transcription factors, in addition to TCP transcription factors, interacted with TIE1 (fig. S6A) (*29*). To test whether TIE2 can interact with type B ARRs, we first cloned seven type B ARRs genes: *ARR1*, *ARR2*, *ARR10*, *ARR11*, *ARR12*, *ARR14*, and *ARR18*. Yeast two-hybrid assays were performed using TIE2 as bait and type B ARRs as prey. The results showed that ARR1, ARR2, and ARR14 interacted strongly with TIE2, while ARR10 and ARR11 interacted weakly with TIE2 (fig. S6B). We next confirmed the interactions between TIE2 and type B ARRs using type B ARRs as the bait and TIE2 as the prey. The results showed that ARR11, ARR14, and ARR18 interacted with TIE2 (fig. S6C). We then used firefly luciferase complementation imaging assays to test whether TIE2 can interact with type B ARRs in planta. Fluorescence was clearly detected following cotransformation of nLUC-TIE2 with cLUC-ARR1, cLUC-ARR2, cLUC-ARR10, cLUC-ARR11, cLUC-ARR12, cLUC-ARR14, and cLUC-ARR18, while the cotransformation of nLUC-TIE2 with cLUC-ARR3 (type A ARR) and the other control cotransformation showed no fluorescence (Fig. 4, A to D, and fig. S6, D to F). The results suggest that TIE2 interacts with these type B ARRs in vivo. Firefly luciferase complementation imaging assays also showed that TIE1 interacted with ARR1 in planta (fig. S6G). To further verify the interactions between TIE2 and ARR1/ARR2, we performed coimmunoprecipitation (co-IP) assays by transiently expressing Myc-tagged TIE2 and Flag-tagged ARR1 or ARR2 in *Nicotiana benthamiana* or *Arabidopsis* protoplasts. The results showed that TIE2 pulled down ARR1 and ARR2 in both expression systems (Fig. 4, E and F, and fig. S7). These results indicate that TIE2 interacts with ARR1 and ARR2 in vivo.

To determine the domains involved in the interaction between TIE2 and type B ARRs, we divided TIE2 into the N-terminal domain (TIE2-N, 1 to 125) including the helix region and the C-terminal domain (TIE2-C, 126 to 178) containing the EAR motif (Fig. 4G). ARR2 was divided into three parts, including ARR2-DDK (1 to 144), ARR2-Ac-M (145 to 268), and ARR2-Q (269 to 664; Fig. 4G). Yeast two-hybrid assays showed that the N terminus of TIE2 interacted with the glutamine-rich domain of ARR2 (Fig. 4H).

To investigate the effect of TIE2 interaction with type B ARRs, we generated the reporter 35S-REN-ARR15pro-LUC, in which the promoter of type A *ARR15* (known to be directly targeted by type B ARRs) was used to drive the *LUC* gene, and *REN* was used as an internal control (Fig. 4I). The reporter was cotransformed with 35S-ARR1, in which the *ARR1* genes was driven by a CaMV 35S promoter, leading to clear activation of *LUC* expression, as expected (Fig. 4I). However, 35S-TIE2, in which *TIE2* was driven by a CaMV 35S promoter, repressed the activation of the reporter by ARR1, while 35S-TIE2mEAR (carrying mutations in the EAR motif) did not (Fig. 4I). To determine whether the EAR motif mutations in the TIE2mEAR could affect the interaction between TIE2mEAR and ARR1, we first performed yeast two-hybrid assay and found that TIE2mEAR interacted with both ARR1 and ARR2 as TIE2 (fig. S8A). Co-IP analysis confirmed that TIE2mEAR interacted with ARR1 in vivo using the *Arabidopsis* transient expression system (fig. S8B), suggesting that the result that TIE2mEAR could not repress the transactivation activity of ARR1 was not due to the compromised interaction between TIE2mEAR and ARR1. We further showed that TIE2 repressed the transactivation activity of ARR2, while mutations in TIE2mEAR significantly decreased the repression activity of TIE2 (fig. S9). These results indicate that the interaction of TIE2 with ARR1 or ARR2 suppresses the transactivation activity of ARR1 or ARR2, and the EAR motif of TIE2 is required for its repression activity.

The results described above indicate that TIE2 interacts with type B ARR transcription factors via its N terminus, whereas its C terminus is involved in repressing their activity. We hypothesized that TIE2 could act as a bridge, using its N terminus to connect with type B ARRs and using its C-terminal EAR motif to link with TPL/TPR co-repressors. Compromised expression of *TIE1* and *TIE2* could lead to de-repression of type B ARRs in *tie1-1 tie2-1*, causing excessive cytokinin signaling and shorter roots. To confirm this hypothesis, we artificially fused ARR1 with the C terminus of TIE2 by generating ARR1pro-ARR1-TIE2C, ARR2pro-ARR2-TIE2C, or TIE2pro-ARR1-TIE2C, in which the *ARR1-TIE2C* or *ARR2-TIE2C* fusion gene was driven by the *ARR1*, *ARR2*, or *TIE2* promoter (Fig. 4J). We expected the repressive versions of ARR1-TIE2C and ARR2-TIE2C to compete with endogenous type B ARRs, inhibit their activity, and thus rescue the root elongation defects in *tie1-1 tie2-1* (*34*). We transformed ARR1pro-ARR1-TIE2C, ARR2pro-ARR2-TIE2C, or TIE2pro-ARR1-TIE2C into the double mutant *tie1-1 tie2-1*. As expected, transformation with ARR1pro-ARR1-TIE2C, ARR2pro-ARR2-TIE2C, or TIE2pro-ARR1-TIE2C rescued the short root phenotype and the cell elongation in the EZ and DZ of *tie1-1 tie2-1* (Fig. 4, J to M). These results strongly suggest that TIE2 acts as a repressor to suppress the activity of type B ARRs.

Cytokinin signaling is significantly enhanced in the *tie1-1 tie2-1* double mutant

To provide more evidence showing that TIE1 and TIE2 repress the activity of type B ARRs and regulate the cytokinin response, we carried out RNA sequencing (RNA-seq) using the roots of 7-day-old *tie1-1 tie2-1* and wild-type control seedlings. The transcriptome data showed that 1357 differentially expressed genes (DEGs; false discovery rate < 0.05; fold change, >2.0 or <−2.0), including 776 up-regulated genes and 581 down-regulated genes, were identified between *tie1-1 tie2-1* and the wild-type controls (fig. S10A and data files S1 and S2). Among these DEGs, 468 genes (34% DEGs) were directly targeted by ARR1, ARR10, or ARR12 (fig. S10B) (*15*). Gene Ontology (GO) analysis showed that genes related to pathways including root hair development, cytokinin-activated signaling pathway, and response to cytokinin were highly enriched in the DEGs (fig. S10C). Venn diagram analysis showed that many DEGs overlapped with the golden list of genes regulated by cytokinin (*35*), as well as 813 common target and 1713 union target genes identified by integrating type B ARR chromatin immunoprecipitation sequencing (ChIP-seq) analysis with cytokinin-regulated gene expression (fig. S10, D to G) (*15*). Among them, many type B ARR direct target genes including type A *ARR16*, *ARR15*, *ARR3*, and *ARR7* were significantly up-regulated in *tie1-1 tie2-1* (data file S3 to S5). Heatmap analysis suggested that the expression levels of 10 type A *ARR* genes known to be directly targeted by type B ARRs were increased in *tie1-1 tie2-1* (Fig. 5A). Motif analysis showed that the core motifs bound by type B ARR or TCP transcription factors were enriched in the 500-bp promoter region upstream of the start codon ATG from the 776 up-regulated genes (fig. S10, H and I) (*36*, *15*). To verify the RNA-seq data, we performed quantitative real-time polymerase chain reaction (qRT-PCR) using cDNA from the roots of 3- or 7-day-old seedlings to measure the expression levels of the 10 type A *ARR* genes directly targeted by

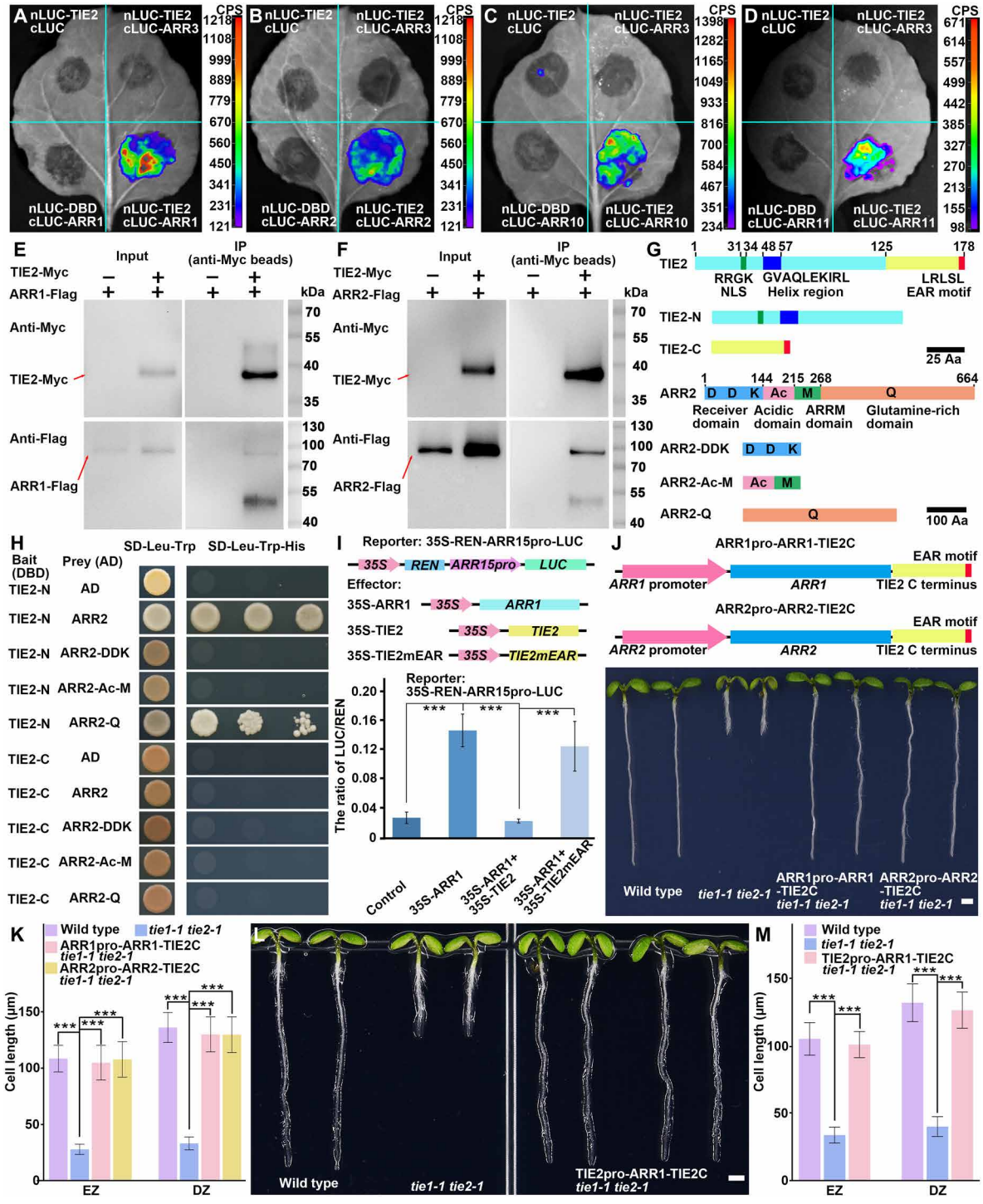

Fig. 4. TIE2 repressed the transactivation activity of ARR1 and ARR2 by directly interacting with them. (**A** to **D**) Firefly luciferase complementation assays showed that TIE2 interacted with ARR1, ARR2, ARR10, and ARR11 in planta. cLUC and cLUC-ARR3 were used as negative controls. (**E** and **F**) Co-IP assays confirmed that TIE2 interacted with ARR1 or ARR2 in vivo. (**G** and **H**) The truncated protein analysis showed that the N terminus of TIE2 interacted with the glutamine-rich domain of ARR2 protein. (G) A schematic diagram of the truncated fragments of TIE2 and ARR2 used in the yeast two-hybrid assays in (H). (**I**) TIE2 repressed the transactivation activity of ARR1, and the EAR motif was required for the repression activity of TIE2. The reporter 35S-REN-ARR15pro-LUC and other constructs in the upper schematic diagrams were used in the *Arabidopsis* protoplast assays shown in the bottom. The data are means (±SD) of three replicates. (**J** and **K**) Expression of an artificial protein consisting of ARR1 or ARR2 fused with the C terminus of TIE2 using the promoter of *ARR1* or *ARR2* rescued the short roots and the cell elongation in the EZ and DZ of *tie1-1 tie2-1*. Data are means ± SD ($n = 40$) of three independent experiments. (**L** and **M**) Expression of an artificial protein consisting of ARR1 fused with the C terminus of TIE2 using the *TIE2* promoter rescued the short roots and the cell elongation in the EZ and DZ of *tie1-1 tie2-1*. Data are means ± SD ($n = 48$) of three independent experiments. Scale bar, 1 mm (J and L). Student's *t* test was used for significance testing, ***$P < 0.001$ in (I, K, and M).

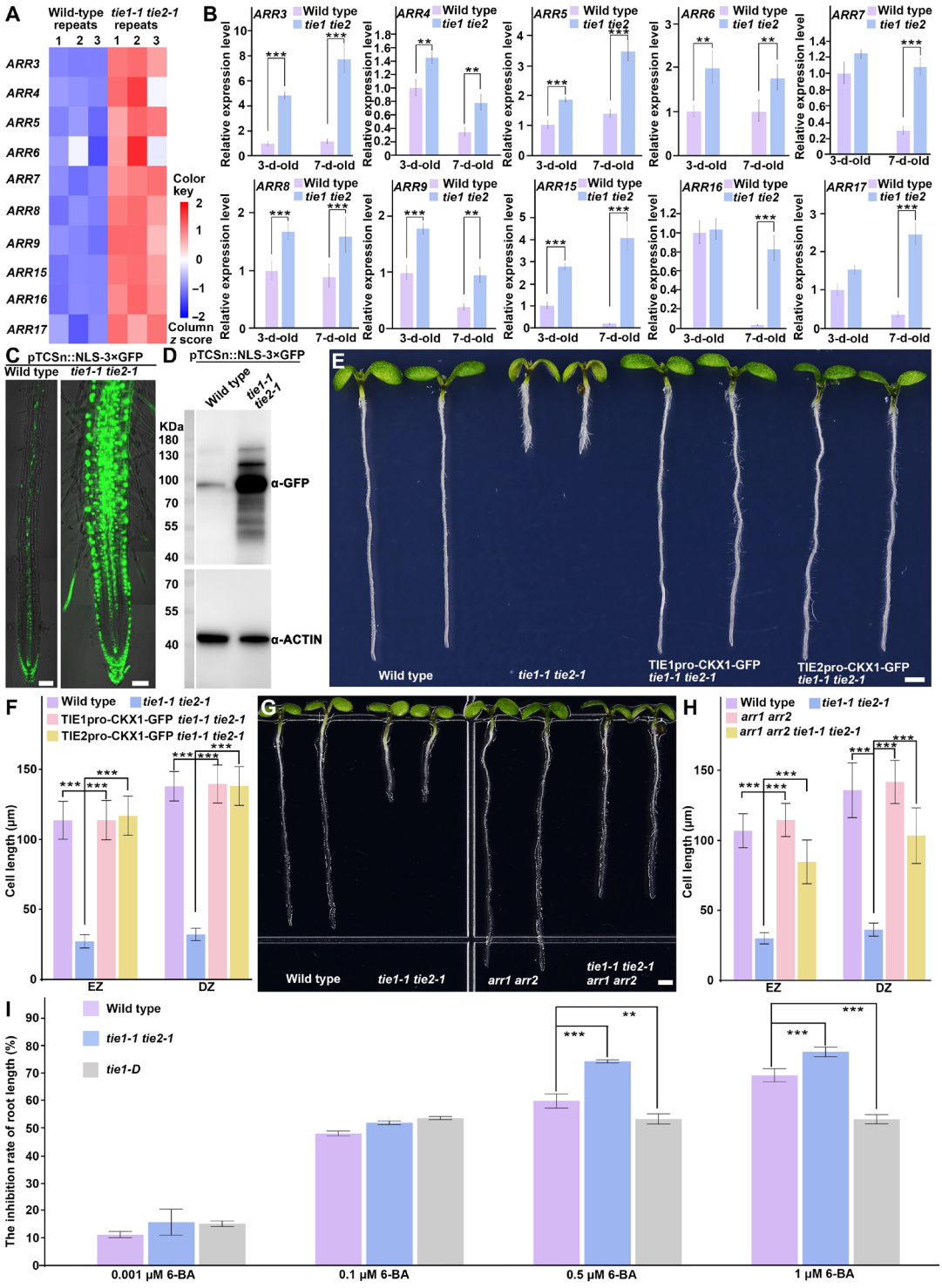

Fig. 5. Disruption of *TIE1* and *TIE2* in *tie1-1 tie2-1* enhanced cytokinin signaling. (**A**) Heatmap analysis of the FPKM (fragments per kilobase million) of type A *ARRs* directly regulated by type B ARRs. (**B**) Real-time PCR confirmation of the expression level of type A *ARRs* in *tie1-1 tie2-1* and wild-type roots. The data are means (±SD) of three replicates. (**C**) TCSn::NLS-3×GFP marker was introduced in *tie1-1 tie2-1*. The GFP signal was significantly increased in the EZ and DZ of roots in *tie1-1 tie2-1*, while the signal in the root meristem of *tie1-1 tie2-1* was comparable to that of wild-type control. (**D**) The Western blot confirmed that the expression of the TCSn::NLS-3×GFP marker was significantly induced in the roots of *tie1-1 tie2-1*. (**E** and **F**) Expression of *CKX1* driven by the *TIE1* or *TIE2* promoter in *tie1-1 tie2-1* rescued the short root phenotype and the cell elongation in the EZ and DZ. Data are means ± SD ($n = 30$) of three independent experiments. (**G** and **H**) Disruption of *ARR1* and *ARR2* rescued the short root phenotype and the cell elongation in EZ and DZ of *tie1-1 tie2-1*. Data are means ± SD ($n = 40$) of three independent experiments. (**I**) The inhibition rate of root length of 7-day-old wild type, *tie1-1 tie2-1*, and *tie1-D* treated with 6-BA. Data are means ± SD ($n = 20$) of three independent experiments. Scale bars, 0.1 mm (C) and 1 mm (E and G). Student's *t* test was used for significance testing in (B, F, and H). Two-way analysis of variance (ANOVA) and Bonferroni test were used for statistical analysis in (I). $^{**}P < 0.01$ and $^{***}P < 0.001$ in (B, F, H, and I).

type B ARRs. The results indicated that the expression levels of the tested type A *ARR* genes in the roots of 3- and/or 7-day-old *tie1-1 tie2-1* seedlings were significantly higher than those in the roots of corresponding wild-type seedlings (Fig. 5B), consistent with the RNA-seq data.

To further demonstrate that disruption of the repressors TIE1 and TIE2 leads to activation of cytokinin signaling in roots, we introduced the TCSn::NLS-3×GFP marker, which indicates cytokinin signaling, into *tie1-1 tie2-1* (*37*). Fluorescence observation and Western blotting showed that the GFP protein expression level of *tie1-1 tie2-1* was much higher than that of the wild-type controls (Fig. 5, C and D). We further generated the constructs TIE1pro-CKX1-GFP and TIE2pro-CKX1-GFP, in which *CKX1* (encoding a cytokinin oxidase involved in cytokinin degradation) was driven by the *TIE1* promoter or *TIE2* promoter, respectively. We transformed the constructs into *tie1-1 tie2-1* to decrease the cytokinin input. The results showed that transformation with either TIE1pro-CKX1-GFP or TIE2pro-CKX1-GFP rescued the shorter root phenotype and the cell elongation in the EZ and DZ of *tie1-1 tie2-1* (Fig. 5, E and F). To examine whether the short root phenotype of *tie1-1 tie2-1* could be dependent on the function of type B ARRs, we performed genetic interaction between *tie1-1 tie2-1* and *arr1 arr2*. The results showed that the disruption *ARR1* or *ARR2* in the triple *tie1-1 tie2-1 arr1* or *tie1-1 tie2-1 arr2* mutants weakly rescued the short root phenotype of *tie1-1 tie2-1* (fig. S10, J and K), whereas the quadruple mutant *tie1-1 tie2-1 arr1 arr2* produced roots with the length comparable to that of wild-type control (fig. S10, J and K, and Fig. 5G). The cell elongation in the EZ and DZ was also rescued in *tie1-1 tie2-1 arr1 arr2* (Fig. 5H). These results demonstrate that the short root phenotype of *tie1-1 tie2-1* is caused by enhanced cytokinin signaling through the release of suppression of type B ARRs, and TIEs are strong negative regulators of cytokinin signaling.

To provide more evidences to support that TIEs negatively regulate cytokinin signaling, we tested the expression of type A *ARR* genes including *ARR3*, *ARR4*, *ARR7*, *ARR8*, *ARR9*, and *ARR15* in the seedlings of *tie1-1 tie2-1*, the *TIE1* overexpression line *tie1-D*, and wild-type control with or without the treatment of cytokinin. The results showed that these type A *ARR* genes were induced more significantly in *tie1-1 tie2-1* but less in *tie1-D* when compared to the induction in wild-type control by cytokinin (fig. S11, A to F), suggesting that *tie1-1 tie2-1* was more sensitive to cytokinin, while *tie1-D* is less sensitive to cytokinin. We next treated wild-type control, *tie1-1 tie2-1*, and *tie1-D* with cytokinin in different concentrations for evaluation of root elongation. The inhibition rate of root length by cytokinin is lower in *tie1-D* but higher in *tie1-1 tie2-1*, when compared with that in wild-type control (Fig. 5I), again suggesting that *tie1-D* is resistant to cytokinin, while *tie1-1 tie2-1* is more sensitive to cytokinin. We further observed the length of root meristem. The results showed that cytokinin treatment significantly inhibited root meristem. However, the inhibition of root meristem was comparable between wild type and *tie1-1 tie2-1* (fig. S11G), suggesting that the sensitivity of root meristem to cytokinin is not changed in *tie1-1 tie2-1*. We lastly treated pTCSn::NLS-3×GFP in the wild-type and in *tie1-1 tie2-1* background with cytokinin. The observation of the GFP fluorescence showed that the increased GFP fluorescence is similar in wild type and *tie1-1 tie2-1* in the root meristem region (fig. S11, H to K), consistent with the result that the inhibition of root meristem by cytokinin was similar in wild type and *tie1-1 tie2-1* (fig. S11G). However, the GFP fluorescence in *tie1-1 tie2-1* was increased more significantly than that in wild-type background in the DZ after cytokinin treatment (fig. S11, L to O). These results further demonstrate that TIE1 and TIE2 promote root elongation by repressing cytokinin signaling.

TIE1 and *TIE2* are directly up-regulated by type B ARR1

In the auxin signaling pathway, EAR motif–containing transcriptional repressors are encoded by *AUX/IAA* genes, which are directly up-regulated by the key transcription factors known as auxin response factors (ARFs). AUX/IAA proteins, in turn, repress the activity of ARFs by directly interacting with them, thus forming an elegant negative feedback loop to suppress activated auxin signaling (*23*). The interactions between type B ARRs and EAR motif–containing TIE2 strongly imply that a similar feedback loop could prevent persistent cytokinin signaling. To test this hypothesis, we first treated 7-day-old seedlings with cytokinin for a short period of time (45 min) to test whether cytokinin induced expression of *TIE1* and *TIE2*. The results showed that the expression levels of *TIE1*, *TIE2*, and the positive control *ARR15* were significantly increased by cytokinin treatment (Fig. 6, A to C). To further determine whether the induction of *TIE1* and *TIE2* by cytokinin could be a primary response, we treated the seedlings with cytokinin and cycloheximide (CHX; a protein synthesis inhibitor). Following treatment with CHX, *TIE1*, *TIE2*, and *ARR15* were still induced by cytokinin treatment, suggesting that *TIE1* and *TIE2* are primary genes regulated by cytokinin signaling as *ARR15* (Fig. 6, A to C). We then searched the promoter regions of *TIE1* and *TIE2* and *ARR15* for type B ARR binding sites using AthaMap software (*38*), which identified dozens of potential cis-elements recognized by type B ARRs in the 1000-bp promoter regions upstream of the translation initiation sites of *TIE1*, *TIE2*, and the positive control *ARR15* (fig. S12). We next searched the published ARR1 ChIP-seq data (*15*, *16*) and found obvious binding signals in the promoter regions of *TIE1*, *TIE2*, and *ARR15*, which increased in binding intensity following cytokinin treatment (Fig. 6, D to F). ChIP-PCR confirmed that ARR1 was significantly enriched near cis-elements bound by ARR1 in the promoter of *TIE2* (Fig. 6G). Electrophoretic mobility shift assay (EMSA) showed that ARR1 directly bound to the cis-elements in the promoter of *TIE2* in vitro (Fig. 6H). We further generated the reporters 35S-REN-TIE1pro-LUC and 35S-REN-TIE2pro-LUC, in which the *LUC* gene was driven by the *TIE1* promoter or *TIE2* promoter, respectively, and *REN* was used as an internal control. We cotransformed 35S-ARR1 with either 35S-REN-TIE1pro-LUC, 35S-REN-TIE2pro-LUC, or the positive control 35S-REN-ARR15pro-LUC. The *LUC* reporter was significantly activated by ARR1 following cotransformation with each of the three tested combinations (Fig. 6, I to K). These results demonstrate that ARR1 promotes the expression of *TIE1* and *TIE2* by directly binding to their promoters, thus forming an elegant negative feedback loop to finely regulate cytokinin signal output.

It is reported that cytokinin inhibits root elongation by promoting ethylene biosynthesis (*39*). Our GO analysis showed that genes related to ethylene pathway were highly enriched in the DEGs (fig. S10C). To determine whether TIE1 and TIE2 could affect ethylene biosynthesis or signaling, we first searched the reported ChIP-seq data of ethylene insensitive 3 (EIN3), a key positive regulator of ethylene signaling (*40*), and found that EIN3 may bind to the promoter region of *TIE1* but not *TIE2* (fig. S13, A and B). To test whether ethylene could induce *TIE1* and *TIE2* rapidly, we treated wild-type seedlings with the ethylene precursor 1–aminocyclopropane-1-carboxylic acid (ACC) in a short time. *TIE1* and *TIE2* were not

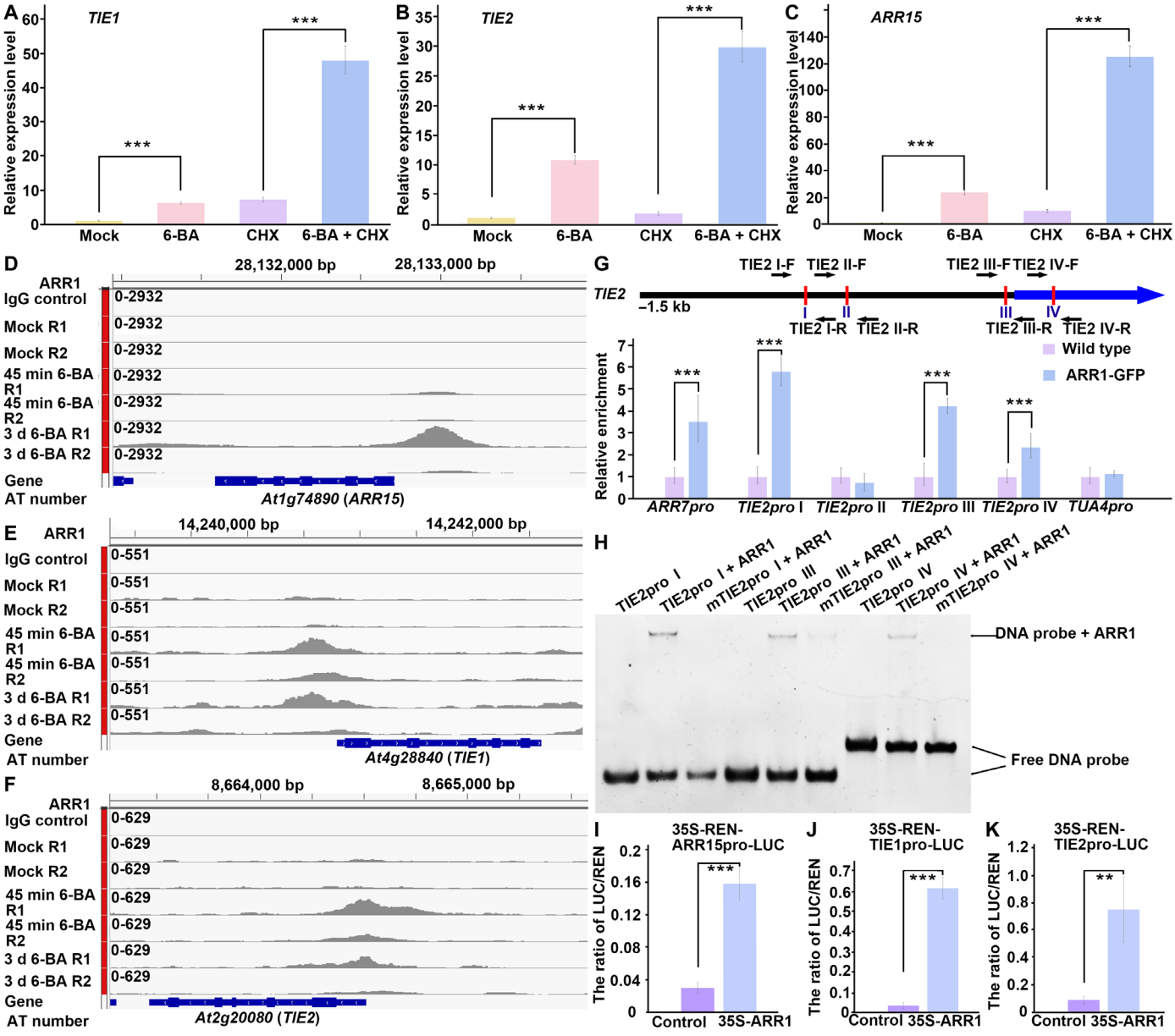

Fig. 6. *TIE1* and *TIE2* are directly induced by *ARR1*. (**A** to **C**) *TIE1* and *TIE2* are rapidly up-regulated by cytokinin treatment. The 7-day-old seedlings were treated with mock, 6-BA, CHX, or 6-BA and CHX for 45 min. The type A *ARR15* gene was used as the positive control. The data are means (± SD) of three replicates. (**D** to **F**) Analysis of ChIP-seq raw reads previously reported at the loci of the *ARR15*, *TIE1*, and *TIE2* genes (*15*). The peaks in the graphs indicate the binding of type B ARR1. (**G**) ChIP-PCR analysis confirmed that ARR1 directly bound to the promoter of *TIE2*. Top: The schematic diagram shows the positions of cis-elements and primers used in the ChIP-PCR in the upstream region of *TIE2*. The vertical red lines indicate the potential ARR1-binding site 5′-(A/G)GAT(T/C)-3′. The blue arrow indicates *TIE2*. *TIE2*-I: −918 to −914 bp; *TIE2*-II: −737 to −733 bp; *TIE2*-III: −35 to −31 bp; *TIE2*-IV: 164 to 168 bp. The black arrows represent the primers used for ChIP-PCR. Five-day-old wild-type and 35S-GFP-ARR1 seedlings were used. The relative enrichment of the wild-type control was set to 1.0. The *ARR7* and *TUA4* transposon loci were used as positive or negative controls. The data are means (± SD) of three replicates. (**H**) EMSA experiments confirm that ARR1 directly binds to the promoter of *TIE2* in vitro. (**I** to **K**) The transient assays showed that ARR1 directly activated the expression of *TIE1* and *TIE2* in *Arabidopsis* protoplasts. The data are means (± SD) of three replicates. Student's *t* test was used for significance testing, $^{**}P < 0.01$ and $^{***}P < 0.001$ in (A to C, G, and I to K).

significantly induced by ACC treatment, whereas the positive control *ERF1* was significantly up-regulated by ACC treatment (fig. S13, C to E). We then treated wild type, *tie1-1 tie2-1*, constitutive triple response (*ctr1*), and *EIN3* overexpression line *EIN3ox* with aminoethoxyvinylglycine (AVG), an inhibitor of ethylene biosynthesis (*41*). As expected, the activated ethylene signaling in *ctr1* or *EIN3ox* caused short root phenotype that was not rescued by AVG treatment. However, the short root phenotype of *tie1-1 tie2-1* was almost completely rescued by the treatment with ethylene biosynthesis inhibitor AVG (fig. S14), suggesting that TIE1 and TIE2 do not directly affect ethylene signaling. These results further support that TIE1 and TIE2 repressed type B ARR transcription

factors to finely tune cytokinin signaling and, thus, the production of ethylene.

The quadruple *tie1 tie2 tie3 tie4* mutants produce defective seeds and shorter roots

To overcome the possible redundant roles of *TIEs* and reveal general involvement of *TIEs* in fine-tuning cytokinin signaling during plant development, we generated *tie3-1* null mutant by CRISPR-Cas9 technology and identified a T-DNA insertion mutant *SALK_018686* from public database as *tie4-1* (Fig. 7, A and B). A 5-bp deletion was found in the first exon of *tie3-1* and caused premature termination of TIE3 translation (Fig. 7A), while the T-DNA insert was located at the fourth exon of *TIE4* and disrupted the function of *TIE4* (Fig. 7, B and C). We introduced *tie3-1* and *tie4-1* into *tie1-1 tie2-1* to generate the quadruple mutant *tie1-1 tie2-1 tie3-1 tie4-1* by crossing. We found that most of *tie1-1 tie2-1 tie3-1 tie4-1* seeds did not germinate, indicating that *TIEs* are important for seed viability (Fig. 7, D to F). The few germinated seeds produced seedlings with very short roots or no roots (Fig. 7G). The seedlings frequently produced one cotyledon or cup-shaped cotyledon resembling the phenotypes of *tpl-1* mutant (Fig. 7G) (*42*). To confirm that *TIEs* played redundant roles in seed development, we used CRISPR-Cas9 technology to generate *tie1-2 tie2-2 tie3-2 tie4-2* in which the deletions or insertions were detected in the first exon of each *TIE* gene and disrupted the function of *TIE*s (fig. S15). The new allele of quadruple mutant *tie1-2 tie2-2 tie3-2 tie4-2* also produced a high ratio of defective seeds that did not germinate (Fig. 7, H and I). The few germinated seeds of *tie1-2 tie2-2 tie3-2 tie4-2* also produced the seedlings with short roots, one cotyledon, or fused cotyledon (Fig. 7J). Microscope observation showed that the roots from quadruple mutants produced defective root meristems (Fig. 7, K and L). We further analyzed the root meristem of wild type, *tie1-1 tie2-1*, and *tie1-1 tie2-1 tie3-1 tie4-1* using 5-ethynyl-2′-deoxyuridine (EdU) staining. The results showed that the size of root meristem was comparable between wild type and *tie1-1 tie2-1* (fig. S16, A and B). However, the root meristem in *tie1-1 tie2-1 tie3-1 tie4-1* was severely shortened, and even no root meristem was stained in some lines of *tie1-1 tie2-1 tie3-1 tie4-1* (fig. S16, C and D). These data indicate that TIEs are essential for root development and may have a broad role in different developmental processes by tightly regulating cytokinin signaling.

DISCUSSION

Here, we demonstrate that the EAR motif–containing proteins TIE1 and TIE2 act as transcriptional repressors to strongly inhibit the cytokinin response. The double loss-of-function mutant *tie1-1 tie2-1* displays an excessive cytokinin response and thus produces shorter roots. *TIE1* and *TIE2* have an overlapping expression pattern and are predominantly expressed in the root EZ and DZ. We show that TIE2 is a transcriptional regulator with repression activity that represses the transactivation activity of type B ARR1 by directly interacting with it in vivo. We further demonstrate that *TIE1* and *TIE2* are direct targets of ARR1. ARR1 directly up-regulates the expression of *TIE1* and *TIE2* in the primary response to cytokinin. Our data indicate that TIE1 and TIE2 are key regulators of root elongation that functions by preventing an excessive cytokinin response in the EZ and DZ of roots and reveal a previously unidentified potent negative feedback regulation loop for cytokinin signaling.

EAR motif–containing transcriptional repressors are key factors in several different hormone signaling pathways (*22*–*26*). It is well established that these repressors use the EAR motif to recruit TPL/TPR co-repressors to key transcription factors and dampen signaling pathways (*22*). For example, AUX/IAAs act as transcriptional repressors via their association with TPL/TPR co-repressors using their EAR motifs (*23*). In the absence of auxin, AUX/IAAs function as adaptor proteins connecting TPL/TPRs with ARFs and thus repress the activity of key transcription factors to prevent transcription of auxin-responsive genes. In the presence of auxin, AUX/IAAs are degraded via the 26*S* proteasome, and ARFs are released to activate the expression of auxin-responsive genes, including *AUX/IAAs*. AUX/IAAs, in turn, repress the activity of ARFs in the absence of auxin (*23*). By this mechanism, the auxin response is tightly and elegantly tuned by the release of ARF activity via the degradation of AUX/IAAs in a process dependent on the level of auxin (*23*). Similar molecular mechanisms have been found in the JA and SL signaling pathways (*24*, *25*). In JA signaling, jasmonate zim-domain (JAZ) transcriptional repressors recruit TPL/TPRs through the EAR motif–containing protein NINJA to suppress the activity of JA-responsive transcription factor MYC proteins (*24*). JA promotes the degradation of JAZ and relieves MYC transcription factors to activate JA-responsive genes (*24*). More recently, the EAR motif–containing SMXL and its rice homolog D53 have been shown to interact with TPL/TPRs (*25*, *43*). The degradation of SMXL or D53 transcriptional repressors activates the SL signaling pathway (*25*, *43*). In addition, EAR motif–containing proteins, including AFPs, ERFs, BZR1, and BES1 (BRI1-EMS-suppressor 1), participate in the signaling pathways of ABA, ethylene, and BR hormones (*26*). We demonstrate that the activity of type B ARR transcription factors, which play key roles in cytokinin signaling, is suppressed by the EAR motif–containing proteins TIE2 and TIE1. As we previously demonstrated regarding TIE1, TIE2 has transcriptional repression activity (*29*). Both TIE2 and TIE1 interact with TPL/TPR co-repressors using the C-terminal EAR motif (*29*). Our data indicate that type B ARRs interact with the N-terminal region of TIE2, suggesting that TIE2 acts as a bridge connecting TPL/TPRs with type B ARRs. Disruption of *TIE1* and *TIE2* in the double mutant *tie1-1 tie2-1* leads to an excessive response to cytokinin in the roots. These data suggest that the type B ARR transcription factors–TIE1/TIE2 adaptor proteins–TPL/TPR co-repressors modules are parallel to ARFs-AUX/IAAs-TPL/TPRs. The difference between these two kinds of modules is that cytokinin can activate unphosphorylated type B ARRs in the nuclei to initiate the cytokinin response, whereas auxin promotes the degradation of AUX/IAAs to release the activity of ARFs. We previously showed that TIE1 is an unstable protein, and we demonstrated that TIE1 degradation is mediated by RING-like E3 ligase TEARs (*31*), but we do not know yet whether or how cytokinin mediates the degradation of TIE1 and TIE2 to relieve the activity of type B ARRs. However, it has been reported that the F-box protein KMD mediates the degradation of type B ARRs (*20*), leading to disassembly of the modules.

TIEs also interact with other transcription factors including TCP transcription factors. The quadruple mutants *tie1-1 tie2-1 tie3-1 tie4-1* and *tie1-2 tie2-2 tie3-2 tie4-2* produce one cotyledon or cup-shaped cotyledon, resembling the phenotype of *topless-1* (*tpl-1*) and overexpression of microRNA319-resistant *TCP4* (*42*, *44*), suggesting that TIEs may act as bridges to connect TCPs and TPL/TPR co-repressors in the control of the cotyledon and leaf development, as well as shoot branching (*29*, *30*, *42*). Here, disruption of type B ARRs

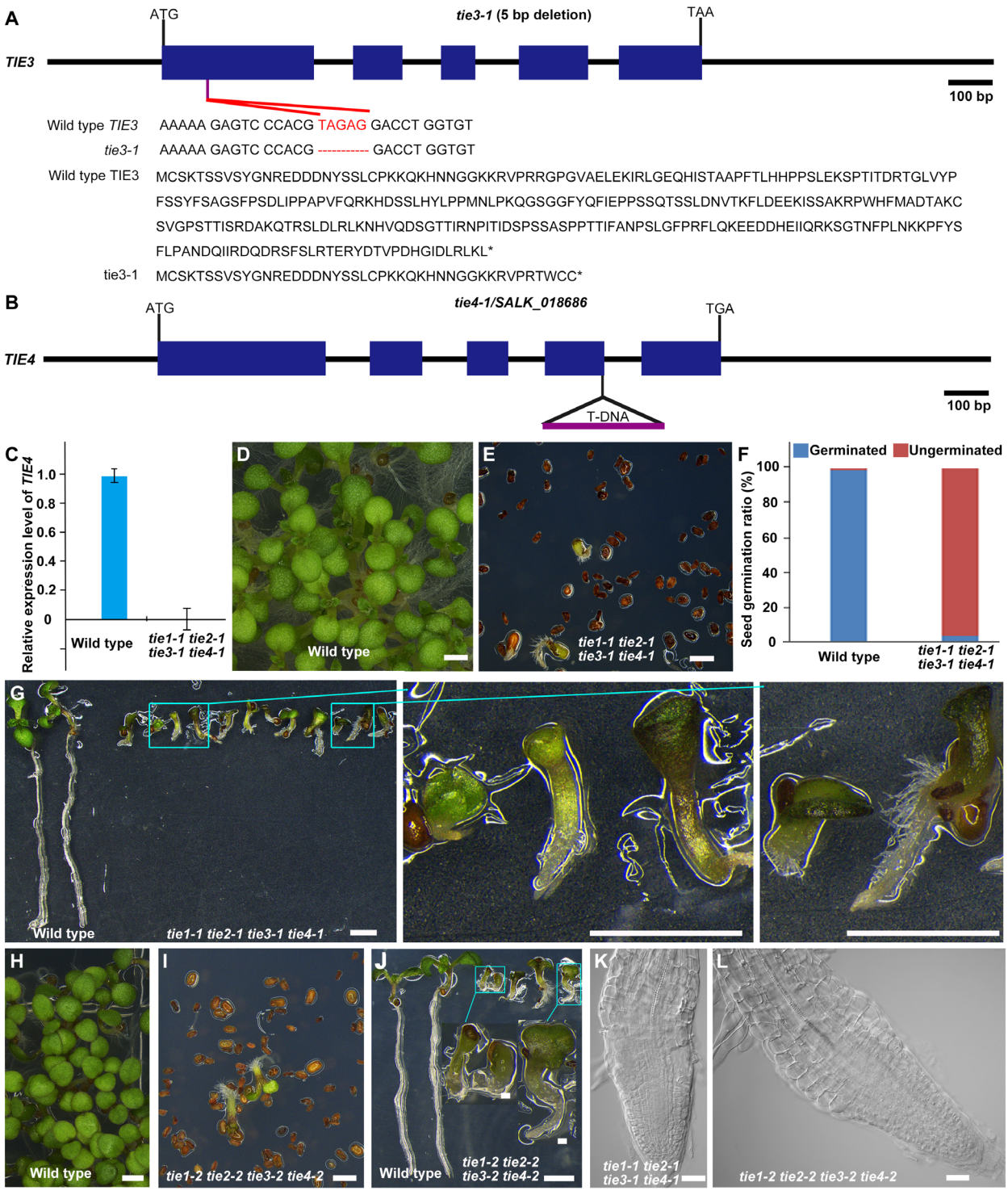

Fig. 7. The *tie1 tie2 tie3 tie4* quadruple mutants produce defective seeds and shorter roots. (**A** and **B**) Schematic diagram of *tie3-1* and *tie4-1* mutants. (**A**) A 5-bp deletion in the first exon of *TIE3* was created by CRISPR-Cas9 technology in *tie3-1*. (B) T-DNA was inserted in the fourth exon of *TIE4* in *tie4-1*. (**C**) The relative expression level of *TIE4* in *tie1-1 tie2-1 tie3-1 tie4-1*. (**D** and **E**) The seed germination of wild type (D) and *tie1-1 tie2-1 tie3-1 tie4-1* (E). (**F**) Seed germination analysis of wild type and *tie1-1 tie2-1 tie3-1 tie4-1*. (**G**) Six-day-old seedlings of wild type and *tie1-1 tie2-1 tie3-1 tie4-1*. The right pictures of (G) are the close-up views of *tie1-1 tie2-1 tie3-1 tie4-1* seedlings. (**H** and **I**) Seed germination of wild type (H) and *tie1-2 tie2-2 tie3-2 tie4-2* (I). (**J**) Six-day-old seedlings of wild type and *tie1-2 tie2-2 tie3-2 tie4-2*. The inset pictures in (J) are the close-up views of *tie1-2 tie2-2 tie3-2 tie4-2* seedlings. (**K** and **L**) Differential interference contrast (DIC) observation of roots from *tie1-1 tie2-1 tie3-1 tie4-1* (K) and *tie1-2 tie2-2 tie3-2 tie4-2* (L). Scale bars, 1 mm (D, E, and G to J), 0.1 mm [inset of (J)], and 50 μm (K and L).

in the quadruple mutant *tie1-1 tie2-1 arr1 arr2* or by expressing ARR2pro-ARR2-TIE2C or TIE2pro-ARR1-TIE2C in *tie1-1 tie2-1* rescued the short root phenotype, suggesting that TIEs control root elongation mainly by repressing the activity of type B ARR transcription factors. However, in our RNA-seq data using the root tissues as materials, the promoter analysis of up-regulated genes in *tie1-1 tie2-1* showed that the core TCP-binding motif was also enriched in addition to the core type B ARR-binding motif, suggesting that TIEs may also regulate other signaling pathways in the control of root development.

Cytokinin plays critical roles in diverse processes in plant development. The tight control of cytokinin signal output is essential for developmental plasticity during adaptation to different environmental conditions (*12*, *13*). Type B ARRs are key transcription factors that govern the primary cytokinin signal output by regulating the transcriptome in response to cytokinin (*15*, *17*). Thus, fine regulation of type B ARR transactivation activity is very important for plant growth and development. The activity of type B ARRs is tightly controlled by different mechanisms. For example, type A ARRs are well-known repressors of type B ARRs that function in a negative feedback loop (*8*). In this negative feedback loop, type B ARRs rapidly induce the expression of type A *ARRs* in the primary cytokinin response, and type A ARRs, in turn, indirectly suppress the activity of type B ARRs, possibly by competing with them for the phosphate relayed from AHP1 to AHP5 (*45*, *46*). Although type A ARRs were thought to be the most important factors involved in dampening the cytokinin response in a feedback loop until now, the high-order type A *ARR* sextuple mutant *arr3,4,5,6,8,9* does not display significant morphological defects (*8*, *46*). We show that *TIE1* and *TIE2* are also up-regulated in the primary cytokinin response. TIE1 and TIE2 suppress the cytokinin response by directly interacting with type B ARRs. Compromised TIE1/TIE2 function in the double mutant *tie1-1 tie2-1* causes severely shortened roots, and the quadruple *tie1 tie2 tie3 tie4* mutants produced even shorter or no root phenotype. These indicate that the negative feedback loop mediated by TIEs is pivotal for controlling appropriate cytokinin signal output during plant development.

Cytokinin plays a critical role in flexible root growth and development by influencing cell division and differentiation in different root zones (*2*). During embryogenesis, cytokinin participates in establishment of the SCN (*47*). At the postembryogenesis stage, cytokinin does not affect the SCN, but it negatively regulates the size of the root meristem (*5*, *48*). In this process, ARR1 is activated by the cytokinin signal to promote the expression of SHORT HYPOCOTYL 2 (*SHY2*) and thus inhibits auxin transport while simultaneously enhancing auxin degradation by increasing the expression of GRETCHEN HAGEN 3.17 (*GH3.17*), resulting in an auxin minimum in the TZ, which increases the rate of cell differentiation in the root meristem

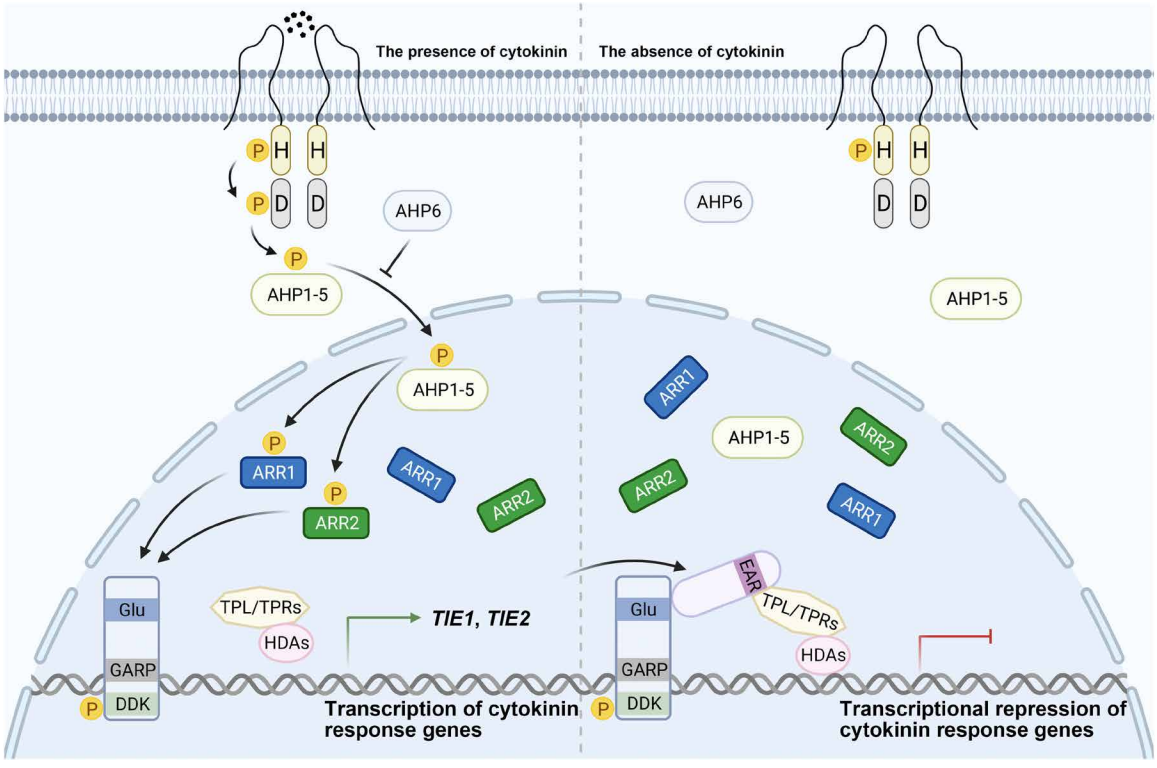

Fig. 8. A working model of *TIE1* and *TIE2* in the suppression of cytokinin signaling. In the presence of cytokinin, cytokinin is perceived by AHKs. AHKs are autophosphorylated, and phosphate was transferred to the Asp residue in the receiver domain immediately. AHP1 to AHP5 subsequently relay the phosphate to type B ARRs to activate them. The activated type B ARRs promote the transcription of cytokinin response genes, including *TIE1*, *TIE2*, and type A *ARRs*. TIE1 and TIE2, in turn, act as bridges connecting type B ARRs with TPL/TPR co-repressors and HDAs to suppress the cytokinin response and prevent continuation of the response in the absence of cytokinin. H and D represent the conserved phosphor-accepting histidine and aspartate residues, respectively. P indicates phosphate.

(*48*). On the other hand, cytokinin activates ARR2 that directly promotes the expression of CELL CYCLE SWITCH52 A1 (*CCS52A1*). CCS52A1 acts as a cell cycle switch to stop cell division by promoting the degradation of mitotic regulators (*6*). It is reported that the compromise of cytokinin signaling leads to an enlarged root meristem by delaying cell endoreplication and the first rapid cell elongation at the boundary between the PZ and TZ. However, at the boundary of the TZ and EZ, the second rapid elongation cell with more than twofold length increase is not related to endoreplication but involves actin reorganization. Cytokinin promotes the onset of actin bundling and the second rapid cell elongation by activating type B ARRs (*49*). The negative effect of cytokinin on the size of the root meristem is independent of its positive effect on ethylene biosynthesis. In contrast, cytokinin profoundly affects root elongation in the EZ and DZ by promoting ethylene biosynthesis (*17*, *50*). The application of cytokinin or overexpression of the cytokinin biosynthetic gene ISOPENTENYLTRANS-FERASE (*IPT*) represses root elongation (*51*, *52*), while disruption of cytokinin signaling key component type B *ARR1*, *ARR10*, and *ARR12* in loss-of-function *arr1* and *arr1 arr10 arr12* mutants leads to longer roots (*53*). We found that TIE1 and TIE2 are potent inhibitors of type B ARRs because disruption of TIE1 and TIE2 causes highly increased expression of the cytokinin response marker TCSn::NLS-3×GFP and severely shortened roots caused by the compromised cell elongation in the EZ and DZ. Consistently, the treatment with ethylene biosynthesis inhibitor rescues the short root phenotype, indicating that TIE1 and TIE2 reduce cytokinin sensitivity and thus prevent excessive ethylene biosynthesis to promote cell elongation. However, *tie1-1 tie2-1* did not produce any observed abnormality in the root meristem. This effect can be explained by the high redundant function of TIE family proteins. Our genetic data showed that the disruption of *TIE1*, *TIE2*, *TIE3*, and *TIE4* in the quadruple *tie1 tie2 tie3 tie4* mutants causes severely developmental phenotypes including short root meristem or no roots. It is proposed that cytokinin signaling regulates cell proliferation in the root meristem by mainly controlling rootward auxin transport through the vasculature while regulating cell elongation in the EZ and DZ by mainly controlling shootward auxin transport through the outer cells of the root cap and TZ (*54*). We showed that TIE1 and/or TIE2 was expressed in lateral root cap, epidermis, and vasculature of roots. The fact that the cell elongation in the EZ and DZ, but not cell proliferation, in root meristem was affected in *tie1-1 tie2-1* may be due to the partially activated cytokinin response by loss of TIE1 and TIE2. However, disruption of four *TIEs* leads to a stronger effect on cytokinin signaling, and both the cell proliferation in the root meristem and cell elongation in the EZ and DZ are affected in the quadruple *tie1 tie2 tie3 tie4* mutants.

To summarize the proposed working model for the functions of TIE1 and TIE2 in cytokinin signaling (Fig. 8), in the presence of cytokinin, cytokinin is perceived by AHK receptors, causing autophosphorylation of His residue in AHKs. The phosphate is subsequently transferred to the Asp residue in the receiver domains of AHKs and then relayed by AHP1 to AHP5 to type B ARRs. The type B ARRs are activated by phosphorylation and bind to DNA to regulate the downstream genes including *TIE* genes and type A *ARRs*. TIEs, in turn, connect type B ARRs with TPL/TPR co-repressors, achieving timely suppression of the cytokinin response in the absence of cytokinin (Fig. 8). Future studies should aim to identify the important roles of TIEs in regulating the sensitivity of the different plant organs or cells in response to cytokinin signal.

MATERIALS AND METHODS

Plant materials and growth conditions

The *Arabidopsis* Columbia-0 (Col-0) ecotype type was used. Wild-type, *tie1-1* (*GABI_372F04*), *tie2-1*, and CyclinB1;1:GUS (*55*), TCSn::NLS-3×GFP seeds (*37*), and other plant materials were first sterilized using 75% ethanol for 10 min and then dried by air flow using a clean bench. The dried seeds were sown on half-strength Murashige and Skoog (1/2 MS) medium and were cold-treated for 2 days in a 4°C refrigerator. The plates were then placed in an incubator at 22°C (16-hour white light and 8-hour dark cycle). For the analysis of root length and morphology, the plates were placed vertically in the incubator. Seedlings of *Arabidopsis* or *Nicotiana benthamiana* were grown in soil in a greenhouse at 22°C (16-hour white light and 8-hour dark cycle).

Root observation and phenotype characterization

For differential interference contrast (DIC) microscopy, the roots from seedlings were mounted in chloral hydrate solution (chloral hydrate:water:glycerol = 8:3:1, w/v/v) before observation. The size of the PZ is determined by the cell number from the initial cell to the first elongated cell characterized by the cell length exceeding its width at the boundary between the PZ and the TZ (*56*). The boundary of the TZ and the EZ were defined by the cells' increase in length by more than twofold (*49*). Root elongation is investigated as previously described (*54*). Briefly, cell length is determined on the shootward side of the EZ and DZ around the region of first root hair initiation cell, which is the marker of the boundary between EZ and DZ. ImageJ software is used to analyze the cell length. At least 20 roots were analyzed, and at least three independent experiments were performed. Student's *t* test was used to evaluate the significance.

To test plant response to exogenous cytokinin, wild-type, *tie1-1 tie2-1*, and *tie1-D* seedlings were grown vertically on plates containing the different concentration of 6-benzylaminopurine (6-BA) for 7 days. The seedlings were photographed, and the length of primary roots was measured using ImageJ software. The inhibition rate was calculated by inhibition rate = $(L_0 - L_x)/L_0 \times 100\%$. L_0 means the root length grown under the normal condition. L_x means the root length grown under the respective concentration of 6-BA.

To determine the phenotype of lateral roots, wild-type and *tie1-1 tie2-1* seedlings were grown on vertical plates for different days and then photographed. The number of primary lateral roots was counted, and the length of main roots was measured. The density of lateral roots was calculated by the number of primary lateral roots/the length of the primary roots.

Generation of the *tie2-1*, *tie3-1*, and *tie1-2 tie2-2 tie3-2 tie4-2* mutants using CRISPR-Cas9 technology

To generate *tie2-1* and *tie3-1*, the sgRNA sequence targeting *TIE2* or *TIE3* was synthesized and inserted into the AtU6-26SK vector using Bbs I to generate AtU6-26SK-TIE2 (*57*). The chimeric RNA expression cassette between the Kpn I and Sal I sites in AtU6-26SK-TIE2 was isolated and then cloned into the 35S-Cas9-pCAMBIA1300 vector (*57*).

To generate *tie1-2 tie2-2 tie3-2 tie4-2* mutant, the egg cell–specific promoter-controlled CRISPR-Cas9 system was used (*58*). Briefly, the sgRNA sequence targeting *TIE1*, *TIE2*, *TIE3*, or *TIE4* was cloned into pENTR-MSR vector to generate the construct pENTR-MSR-TIE1, pENTR-MSR-TIE2, pENTR-MSR-TIE3, or pENTR-MSR-TIE4. Next, the pENTR-MSR-TIE1-TIE4 was generated by isocaudamer enzyme

ligation after digesting pENTR-MSR-TIE1 with Kpn I/Spe I and pENTR-MSR-TIE4 with Xba I/Hind III. The construct pENTR-MSR-TIE1-TIE4-TIE3 was generated from pENTR-MSR-TIE1-TIE4 and pENTR-MSR-TIE3 using the same method. Then pENTR-MSR-TIE1-TIE4-TIE3-TIE2 was generated from pENTR-MSR-TIE1-TIE4TIE3 and pENTR-MSR-TIE2. Last, pHEE401E-TIE1-TIE4-TIE3-TIE2 was generated from pHEE401E and pENTR-MSR-TIE1-TIE4-TIE3-TIE2 by Golden Gate Cloning. The constructs were introduced into wild-type *Arabidopsis* by Agrobacteria-mediated transformation to generate *tie2-1*, *tie3-1* or *tie1-2 tie2-2 tie3-2 tie4-2* mutants. The primers used in this study are listed in table S1.

Genotyping and gene expression analysis

To genotype the T-DNA insertion mutant *tie1-1*, the *tie1-1*-F and *tie1-1*-R primers were designed to amplify the wild-type fragment, while the *tie1-1*-R and O8760 primers were used to amplify the T-DNA insertion fragment. To genotype *tie2-1*, the *tie2-1*-F and *tie2-1*-R primers were used to amplify the genomic DNA of *tie2-1*, and the PCR product was sequenced to identify the mutation in *tie2-1*.

For gene expression analysis, 3- or 7-day-old wild-type and *tie1-1 tie2-1* seedlings treated with or without 6-BA were cut and quickly frozen in liquid nitrogen. Total RNA was extracted using the Plant Total RNA Purification Kit (GeneMark, TR02-150), and M-MLV reverse transcriptase (Promega, M170A) was used to synthesize cDNA. RT-qPCR was carried out using SYBR reagent (CWBIO, CW2601M). The RT-qPCR cycle was as follows: 94°C for 20 s, 58°C for 30 s, and 72°C for 30 s.

Generation of binary constructs and plant transformation

For genetic complementation, TIE1pro-F/TIE1pro-R and TIE1geno-F/TIE1geno-R primer pairs were used to amplify the promoter and coding region of *TIE1* from genomic DNA. The PCR fragments were cloned into pENTR/D-TOPO to generate pENTR-TIE1pro-TIE1nsc. TIE1pro-TIE1-GFP was generated by LR reaction between pENTR-TIE1pro-TIE1 and pKGWFS7. The promoter and coding region of *TIE2* were amplified from genomic DNA using TIE2pro-F/TIE2pro-R or TIE2geno-F/TIE2geno-R. The *TIE2* promoter fragment was cloned into the pDONR P4-P1R plasmid by BP reaction to generate TIE2pro-P4-P1R. The coding region of *TIE2* was cloned into pENTR/D-TOPO to generate pENTR-TIE2geno. The *GFP* sequence was amplified from the pK7FWG0 plasmid by GFP-F/GFP-R primers and cloned into the pDONR-P2R-P3 plasmid to generate GFP-P2R-P3. TIE2pro-TIE2-GFP was generated by LR reaction with TIE2pro-P4-P1R, pENTR-TIE2geno, GFP-P2R-P3, and pB7m34GW.

To determine the subcellular localization of TIE2, 35S-GFP-TIE2 was generated by LR reaction between pK7FWG2 and pENTR-TIE2geno. The construct 35S-NLS-RFP as a nuclear marker was cotransformed into tobacco leaves with 35S-GFP-TIE2.

To decrease the cytokinin input in the double mutant *tie1-1 tie2-1*, the TIE1 promoter was amplified using TIE1pro-F/TIE1pro-R primers, and the PCR product was cloned into pDONR P4-P1R by BP reaction to generate TIE1pro-P4-P1R. The *CKX1* gene was amplified from *Arabidopsis* cDNA and cloned into pENTR/D-TOPO to generate pENTR-CKX1. TIE1pro-CKX1-GFP and TIE2pro-CKX1-GFP were generated by LR reaction with TIE1pro-P4-P1R or TIE2pro-P4P1R, respectively, as well as pENTR-CKX1 and GFP-P2R-P3.

To generate ARR1pro-ARR1-TIE2C and ARR2pro-ARR2-TIE2C, the promoter of *ARR1* or *ARR2* was amplified using ARR1pro-F/ARR1pro-R or ARR2pro-F/ARR2pro-R, respectively, and cloned into P4-P1R by BP reaction to generate ARR1pro-P4-P1R or ARR2pro-P4-P1R, respectively. The *ARR1* and *ARR2* coding regions were amplified from genomic DNA using primer pairs ARR1-F/ARR1-R and ARR2-F/ARR2-R, respectively, and then cloned into pENTR/D-TOPO to generate pENTR-ARR1geno and pENTR-ARR2geno, respectively. The TIE2C sequence, encoding the C terminus of TIE2, was amplified using TIE2-C-F/TIE2-C-R primers and cloned into P2R-P3 to generate P2R-P3-TIE2C. ARR1pro-ARR1-TIE2C was generated by LR reaction with ARR1pro-P4-P1R, pENTR-ARR1geno, P2R-P3-TIE2C, and pB7m34GW. ARR2pro-ARR2-TIE2C was generated by LR reaction with ARR2pro-P4-P1R, pENTR-ARR2geno, P2R-P3-TIE2C, and pH7m34GW. TIE2pro-ARR1-TIE2C was generated by LR reaction with TIE2pro-P4P1R, pENTR-ARR1geno, P2R-P3-TIE2C, and pB7m34GW.

The TIE1pro-GUS construct was generated as described previously (*29*). To generate TIE2pro-GUS, a 5104-bp-long *TIE2* promoter was amplified from genomic DNA and cloned into pENTR/D-TOPO to generate pENTR-TIE2pro. TIE2pro-GUS was generated by LR reaction between pKGWFS7 and pENTR-TIE2.

Constructs were transformed into *Agrobacterium tumefaciens* GV3101/pMP90. Plant transformation was performed by an Agrobacterium-mediated floral dip method.

Co-IP and Western blotting

TIE2, *ARR1*, and *ARR2* were amplified from wild-type cDNA and cloned into pENTR/D-TOPO to generate pENTR-TIE1, pENTR-TIE2, pENTR-ARR1, and pENTR-ARR2. To test the interaction between TIE2 and ARR1 or ARR2, TIE2-Myc was generated by LR reaction between pENTR-TIE2 and pK7MYCWG2. ARR1-Flag and ARR2-Flag were produced by LR reaction between pB7FLAGWG2 and pENTR-ARR1 or pENTR-ARR2.

Different combinations were transformed into tobacco leaves or *Arabidopsis* protoplasts. To perform co-IP assays, total protein was extracted with IP buffer [50 mM tris (pH 6.8), 50 mM NaCl, 1 mM EDTA, 1 mM dithiothreitol (DTT), 1 mM phenylmethylsulfonyl fluoride, 1× cocktail, 1‰ MG132, and 1‰ NP-40] and immunoprecipitated using agarose beads conjugated with anti-Myc antibodies (Sigma-Aldrich, E6654) by incubation for 3 hours. Subsequently, the beads were washed five times and boiled with 2× SDS at 100°C for 10 min. The proteins were separated on a 12% polyacrylamide gel electrophoresis (PAGE) gel and transferred onto a polyvinylidene difluoride membrane (Millipore, ISEQ00010). A chemiluminescence detector (Tanon, 5200Multi) was used for detection. Anti-MYC (CWbio, CW0259), horseradish peroxidase (HRP)–conjugated anti-FLAG antibodies (Sigma-Aldrich, A8592), and goat-anti-mouse HRP (CWbio, CW0102S) were used for Western blot assays.

Firefly luciferase complementation imaging assay

To confirm the protein interaction in vivo, nLUC-TIE2 was generated by LR reaction between pENTR-TIE2 and pCAMBIA-nLUC. cLUC-ARRx was generated by LR reaction between pCAMBIA-cLUC and pENTR-ARRx, respectively. cLUC-ARR3 was generated as a negative control. The constructs were transformed into *A. tumefaciens* GV3101. Different combinations were coinfiltrated into tobacco leaves with pCAM-P19. The transformed plants were grown in the dark for 12 hours and then put into a greenhouse with long-day conditions for 48 hours. The isolated tobacco leaves were treated with 1 mM luciferin at the abaxial surface in the dark for 10 min. Luciferase luminescence was detected by a low-light cooled

CCD imaging apparatus (NightOWL II LB 983) with indiGO software.

Yeast two-hybrid assays

ARR10, *ARR11*, *ARR12*, *ARR14*, and *ARR18* were amplified from wild-type cDNA and cloned into pENTR/D-TOPO to generate pENTR-ARRs. Truncated *TIE2* (*TIE2-N* and *TIE2-C*) and *ARR2* (*ARR2-DDK*, *ARR2-Ac-M*, and *ARR2-Q*) were cloned into pENTR/D-TOPO to generate pENTR-TIE2-N, pENTR-TIE2-C, pENTR-ARR2-DDK, pENTR-ARR2-Ac-M, and pENTR-ARR2-Q.

To test the interaction between TIE2 and ARRs, *TIE2* was cloned into pDEST32 (Invitrogen) as bait. AD-ARRs were generated by LR reaction between pENTR-ARRs and pDEST22 as prey. To further confirm the interaction between *TIE2* and type B ARRs, *TIE2* was cloned into pDEST22 as prey, while type B *ARRs* into pDEST32 as bait. To test the interaction between TIE2 and ARR2, pENTR-TIE2-N, and pENTR-TIE2-C were cloned into pEDST32 as bait by LR reaction. pENTR-ARR2-DDK, pENTR-ARR2-Ac-M, and pENTR-ARR2-Q were cloned into pDEST22 as prey by LR reaction. Different combinations of bait and prey constructs were cotransformed into yeast strain AH109. The blank construct pDEST22 was cotransformed with the bait constructs as a negative control. The transformed yeast cells were grown on selective medium supplemented with SD-Leu-Trp-His with or without 2.5 mM 3-AT at 30°C for 3 days.

Transient dual-luciferase reporter assay

To assess the transcriptional repression activity of TIE2 in tobacco leaves, the sequence encoding G4BD-TIE2 (G4BD, GAL4 DNA binding domain) was amplified from the TIE2-pDEST32 construct and cloned into pENTR/D-TOPO to generate pENTR-G4BD-TIE2. 35S-G4BD-TIE2 was generated by LR reaction between pENTR-G4BD-TIE2 and pK2GW7. The sequence encoding G4BD was cloned into pENTR/D-TOPO to generate pENTR-G4BD, and 35S-G4BD was generated by LR reaction between pK2GW7 and pENTR-G4BD. The sequence encoding TIE2mEAR, in which the conserved Leu residues were mutated, was amplified using TIE2-F and TIE2mEAR-R primers, and subsequently cloned into pENTR-D/TOPO to generate pENTR-TIE2mEAR. G4BD-TIE2mEAR was generated by LR reaction between pDEST32 and pENTR-TIE2mEAR. The sequence encoding G4BD-TIE2mEAR was amplified to generate pENTR-BD-TIE2mEAR. 35S-BD-TIE2mEAR was obtained by LR reaction between pK2GW7 and pENTR-BD-TIE2mEAR. Different combinations were coinfiltrated into tobacco leaves with pCAM-P19. The treatment and the detection of luminescence were as described above.

To test the transcriptional repression activity of TIE2 in *Arabidopsis* protoplasts, 35S-G4BD, 35S-G4BD-TIE2, and 35S-G4BD-TIE2mEAR were cloned into pGreen II 62-SK using the FastClone method. *Arabidopsis* protoplasts were prepared as described previously (*59*). Next, the protoplasts were cotransformed with 10 μg of different combinations of plasmids. The transformed protoplasts were collected and resuspended with 1 ml of W5 solution. The LUC/REN ratio was detected by a dual-luciferase reporter assay system (Promega, GLO-MAX 20/20 luminometer) after incubation at room temperature for 16 hours under mild light conditions.

To test whether TIE2 represses ARR1 or ARR2 transactivation activity, the sequences encoding ARR1, ARR2, TIE2, and TIE2mEAR were cloned into pGreen II 62-SK to generate 35S-ARR1, 35S-ARR2, 35S-TIE2, and 35S-TIE2mEAR using the FastClone method. The *ARR15* promoter was amplified by ARR15pro-F and ARR15pro-R and then cloned into pENTR/D-TOPO to generate pENTR-ARR15pro. 35S-REN-ARR15pro-LUC was generated by LR reaction between pENTR-ARR15pro and pGreen II 0800 LUC-GW. The transient expression of different combinations of plasmids and detection of luminescence were performed as described above.

To detect whether TIE2 repressed the transactivation activity of ARR2, the protoplasts coexpressing different combinations of plasmids were collected and resuspended with 100 μl of W5 solution. Ten microliters of 10 mM D-luciferin was mixed with 90 μl of protoplast suspension in 96-well plates. The LUC activity was then detected with Centro XS^3 LB 960 microplate Luminometer continuously in time course.

GUS staining, propidium iodide staining, EdU staining, and GFP observation

TIE1pro-TIE1-GFP and TIE2pro-TIE2-GFP seedlings were fixed in 90% (v/v) acetone for 20 min on ice, washed twice with phosphate buffer, and incubated in GUS staining solution containing 5-bromo-4-chloro-3-indolyl glucuronide at 37°C for 2 hours. The staining solution was then changed to 75% ethanol for decolorizing. The root staining was observed using a Leica M205 FCA stereoscope.

For propidium iodide (PI) staining and GFP observation, *Arabidopsis* seedlings of TIE1pro-TIE1-GFP or TIE2pro-TIE2-GFP were grown vertically on 1/2 MS medium. Roots were stained with PI solution (1 mg/ml; Sigma-Aldrich, P4170) for 30 s. PI staining and GFP were then observed using a confocal laser scanning microscope (Zeiss LSM 710 NLO).

Click-iT EdU Alexa Flour 488 Imaging Kit (Invitrogen, C10337) was used to perform EdU staining. In brief, 5-day-old wild-type and *tie1-1 tie2-1* seedlings were submerged in liquid MS medium containing 20 μM EdU for 30 min. The samples were fixed in phosphate-buffered saline (PBS; pH 7.2 to 7.6) containing 3.7% formaldehyde and 0.1% Triton X-100 for 30 min. The fixative was then removed, and the samples were washed twice with PBS containing 3% bovine serum albumin (BSA). The seedlings were incubated in the Click-iT reaction cocktail for 30 min at room temperature without light. The reaction cocktail was removed, and the samples were washed three times with PBS.

RNA-seq and ChIP-seq analysis

The roots of 7-day-old *tie1-1 tie2-1* and wild-type seedlings were collected for RNA extraction. RNA-seq was carried out by Novogene Corporation with three replicates. RNA-seq libraries consisting of 150-bp paired-end reads were generated on an Illumina NovaSeq 6000 platform. RNA-seq data analysis was described previously (*60*). Briefly, quality control of the raw reads was performed by fastp (0.20.1). The clean reads were mapped to the *Arabidopsis* reference genome (TAIR10) by STAR (2.7.3a). Expression counts were generated by featureCounts in Subread 2.0.1 with default parameters. The R package DEseq2 (1.32.0) was used for differential gene expression analysis. Genes with a Bonferroni-adjusted P value (padj) < 0.05 and a $\log_2$ fold change <−1 or > 1 were considered as significantly DEGs. Volcano plots were generated by R package ggpubr (0.4.0). To perform promoter analysis, motif enrichment was analyzed in the 500-bp promoter regions of up-regulated genes in *tie1-1 tie2-1* using MEME software online (https://meme-suite.org/meme/tools/sea) (*36*).

To determine whether ARR1 could bind to the promoter of *TIE1* and *TIE2*, raw ARR1 ChIP-seq data were downloaded from the Gene Expression Omnibus (accession number GSE94486) (*15*). The analysis

of ChIP-seq data was described previously (*60*). Briefly, the quality control of the raw reads was performed by fastp (0.20.1). The clean reads were mapped to the *Arabidopsis* reference genome TAIR10 by bowtie2 (2.3.5). The unique mapped reads were used for downstream analysis in Samtools (1.9). BigWig files were generated with binSize 10 and the option normalizeUsingBPM using bamCoverage in deepTools (3.3.1). Typical screenshots were captured with Integrative Genomics Viewer (2.6.2). ChIP-seq raw data of EIN3 were downloaded from the Sequence Read Archive (SRA) with the accession number SRA063695 (*40*). The FASTQ files were extracted from SRA files by fasterq-dump (2.9.6) with parameter split-3. The adaptors were removed with trim_galore (0.6.6). The clean reads were mapped the *Arabidopsis* reference genome TAIR10 by bowtie2 (2.3.5). Replicated reads were removed by sambamba (0.8.2). BW files were generated with binSize 10 and normalizeUsinfBPM by bam coverage from deepTools (3.3.1). Typical screenshots were captured with IGV (2.6.2).

ChIP-PCR assay

ChIP experiments were performed as described previously (*59*). The seedlings of 5-day-old wild-type and 35S-GFP-ARR1 seedlings were collected to perform ChIP-PCR. The sonicated chromatin was incubated with 5 μl anti-GFP (Abcam, ab290) at 4°C overnight. Protein A-Sepharose (GE Healthcare 17-1279-01) was used as a negative control and the supernatant after incubation was taken as the input. *TUBULIN ALPHA-4 CHAIN* (*TUA4*) was used as the negative control and *ARR7* as the positive control. The primer pairs used for ChIP-PCR were listed in table S1.

Electrophoretic mobility shift assay

The DNA sequence encoding the ARR1 DNA binding domain (DBD) was cloned into pGEX-4T with an N-terminal glutathione *S*-transferase (GST) tag. The vector was transformed into *Escherichia coli* strain BL21. The bacteria were cultured overnight at 18°C, and proteins were induced by adding isopropyl β-D-1-thiogalactopyranoside (IPTG) to a final concentration of 0.5 mM. The cells were collected and resuspended in binding buffer (PBS, pH 7.3, 1 mM DTT). The target protein was eluted with elution buffer [50 mM tris-HCl, 10 mM reduced glutathione (pH 8.0), and 1 mM DTT] using a GSTrap HP column (Cytiva, 17-5282-01).

The 18- or 30-bp DNA fragments containing ARR1 binding motifs 5′-(A/G)GAT(T/C)-3′ in the *TIE2* promoter region were synthesized. The binding motifs were mutated to AAAAA in the control DNA fragments. Double-stranded DNA was obtained by annealing equimolar concentrations in binding buffer.

To carry out EMSA, the purified GST-ARR1-DBD proteins (about 550 ng) were mixed with double-stranded DNA (200 ng). The mixture was incubated at 4°C for 20 to 30 min and then loaded onto a 7% nondenaturing polyacrylamide gel and subjected to electrophoresis (PAGE) using 0.5× tris-borate EDTA buffer (Sangon, B548102). Electrophoresis was performed at 120 V for 40 hours. Ethidium bromide staining was used to detect DNA under Tanon2500.

SUPPLEMENTARY MATERIALS

Supplementary material for this article is available at https://science.org/doi/10.1126/sciadv.abn5057

View/request a protocol for this paper from *Bio-protocol*.

REFERENCES AND NOTES

1. B. K. Pandey, G. Q. Huang, R. Bhosale, S. Hartman, C. J. Sturrock, L. Jose, O. C. Martin, M. Karady, L. A. C. J. Voesenek, K. Ljung, J. P. Lynch, K. M. Brown, W. R. Whalley, S. J. Mooney, D. B. Zhang, M. J. Bennett, Plant roots sense soil compaction through restricted ethylene diffusion. *Science* **371**, 276–280 (2021).
2. H. Motte, S. Vanneste, T. Beeckman, Molecular and environmental regulation of root development. *Annu. Rev. Plant Biol.* **70**, 465–488 (2019).
3. M. Del Bianco, L. Giustini, S. Sabatini, Spatiotemporal changes in the role of cytokinin during root development. *New Phytol.* **199**, 324–338 (2013).
4. R. Dello Ioio, F. S. Linhares, E. Scacchi, E. Casamitjana-Martinez, R. Heidstra, P. Costantino, S. Sabatini, Cytokinins determine *Arabidopsis* root-meristem size by controlling cell differentiation. *Curr. Biol.* **17**, 678–682 (2007).
5. R. Dello Ioio, K. Nakamura, L. Moubayidin, S. Perilli, M. Taniguchi, M. T. Morita, T. Aoyama, P. Costantino, S. Sabatini, A genetic framework for the control of cell division and differentiation in the root meristem. *Science* **322**, 1380–1384 (2008).
6. N. Takahashi, T. Kajihara, C. Okamura, Y. Kim, Y. Katagiri, Y. Okushima, S. Matsunaga, I. Hwang, M. Umeda, Cytokinins control endocycle onset by promoting the expression of an APC/C activator in *Arabidopsis* roots. *Curr. Biol.* **23**, 1812–1817 (2013).
7. J. C. Montesinos, A. Abuzeineh, A. Kopf, A. Juanes-Garcia, K. Otvos, J. Petrasek, M. Sixt, E. Benkova, Phytohormone cytokinin guides microtubule dynamics during cell progression from proliferative to differentiated stage. *EMBO J.* **39**, e104238 (2020).
8. J. P. To, G. Haberer, F. J. Ferreira, J. Deruere, M. G. Mason, G. E. Schaller, J. M. Alonso, J. R. Ecker, J. J. Kieber, Type-A *Arabidopsis* response regulators are partially redundant negative regulators of cytokinin signaling. *Plant Cell* **16**, 658–671 (2004).
9. R. D. Argyros, D. E. Mathews, Y. H. Chiang, C. M. Palmer, D. M. Thibault, N. Etheridge, D. A. Argyros, M. G. Mason, J. J. Kieber, G. E. Schaller, Type B response regulators of *Arabidopsis* play key roles in cytokinin signaling and plant development. *Plant Cell* **20**, 2102–2116 (2008).
10. H. Sakai, T. Honma, T. Aoyama, S. Sato, T. Kato, S. Tabata, A. Oka, ARR1, a transcription factor for genes immediately responsive to cytokinins. *Science* **294**, 1519–1521 (2001).
11. S. Zhang, L. Huang, A. Yan, Y. Liu, B. Liu, C. Yu, A. Zhang, J. Schiefelbein, Y. Gan, Multiple phytohormones promote root hair elongation by regulating a similar set of genes in the root epidermis in *Arabidopsis*. *J. Exp. Bot.* **67**, 6363–6372 (2016).
12. J. J. Kieber, G. E. Schaller, Cytokinin signaling in plant development. *Development* **145**, dev149344 (2018).
13. J. J. Kieber, G. E. Schaller, Cytokinins. *Arabidopsis Book* **12**, e0168 (2014).
14. C. E. Hutchison, J. J. Kieber, Cytokinin signaling in *Arabidopsis*. *Plant Cell* **14**(Suppl. 1), S47–S59 (2002).
15. M. Xie, H. Chen, L. Huang, R. C. O'Neil, M. N. Shokhirev, J. R. Ecker, A B-ARR-mediated cytokinin transcriptional network directs hormone cross-regulation and shoot development. *Nat. Commun.* **9**, 1604 (2018).
16. Y. O. Zubo, I. C. Blakley, M. V. Yamburenko, J. M. Worthen, I. H. Street, J. M. Franco-Zorrilla, W. Zhang, K. Hill, T. Raines, R. Solano, J. J. Kieber, A. E. Loraine, G. E. Schaller, Cytokinin induces genome-wide binding of the type-B response regulator ARR10 to regulate growth and development in *Arabidopsis*. *Proc. Natl. Acad. Sci. U.S.A.* **114**, E5995–E6004 (2017).
17. Y. O. Zubo, G. E. Schaller, Role of the cytokinin-activated type-B response regulators in hormone crosstalk. *Plants* **9**, 166 (2020).
18. A. P. Mahonen, M. Higuchi, K. Tormakangas, K. Miyawaki, M. S. Pischke, M. R. Sussman, Y. Helariutta, T. Kakimoto, Cytokinins regulate a bidirectional phosphorelay network in *Arabidopsis*. *Curr. Biol.* **16**, 1116–1122 (2006).
19. A. P. Mahonen, A. Bishopp, M. Higuchi, K. M. Nieminen, K. Kinoshita, K. Tormakangas, Y. Ikeda, A. Oka, T. Kakimoto, Y. Helariutta, Cytokinin signaling and its inhibitor AHP6 regulate cell fate during vascular development. *Science* **311**, 94–98 (2006).
20. H. J. Kim, Y.-H. Chiang, J. J. Kieber, G. E. Schaller, SCF^{KMD} controls cytokinin signaling by regulating the degradation of type-B response regulators. *Proc. Natl. Acad. Sci. U.S.A.* **110**, 10028–10033 (2013).
21. M. Ohta, K. Matsui, K. Hiratsu, H. Shinshi, M. Ohme-Takagi, Repression domains of class II ERF transcriptional repressors share an essential motif for active repression. *Plant Cell* **13**, 1959–1968 (2001).
22. S. Kagale, M. G. Links, K. Rozwadowski, Genome-wide analysis of ethylene-responsive element binding factor-associated amphiphilic repression motif-containing transcriptional regulators in *Arabidopsis*. *Plant Physiol.* **152**, 1109–1134 (2010).
23. H. Szemenyei, M. Hannon, J. A. Long, TOPLESS mediates auxin-dependent transcriptional repression during *Arabidopsis* embryogenesis. *Science* **319**, 1384–1386 (2008).
24. L. Pauwels, G. F. Barbero, J. Geerinck, S. Tilleman, W. Grunewald, A. C. Perez, J. M. Chico, R. V. Bossche, J. Sewell, E. Gil, G. Garcia-Casado, E. Witters, D. Inze, J. A. Long, G. De Jaeger, R. Solano, A. Goossens, NINJA connects the co-repressor TOPLESS to jasmonate signalling. *Nature* **464**, 788–791 (2010).
25. L. Wang, B. Wang, H. Yu, H. Guo, T. Lin, L. Kou, A. Wang, N. Shao, H. Ma, G. Xiong, X. Li, J. Yang, J. Chu, J. Li, Transcriptional regulation of strigolactone signalling in *Arabidopsis*. *Nature* **583**, 277–281 (2020).

26. E. Oh, J. Y. Zhu, H. Ryu, I. Hwang, Z.-Y. Wang, TOPLESS mediates brassinosteroid-induced transcriptional repression through interaction with BZR1. *Nat. Commun.* **5**, 4140 (2014).
27. B. Causier, M. Ashworth, W. Guo, B. Davies, The TOPLESS interactome: A framework for gene repression in *Arabidopsis*. *Plant Physiol.* **158**, 423–438 (2012).
28. K. C. Potter, J. Wang, G. E. Schaller, J. J. Kieber, Cytokinin modulates context-dependent chromatin accessibility through the type-B response regulators. *Nat. Plants* **4**, 1102–1111 (2018).
29. Q. Tao, D. Guo, B. Wei, F. Zhang, C. Pang, H. Jiang, J. Zhang, T. Wei, H. Gu, L.-J. Qu, G. Qin, The TIE1 transcriptional repressor links TCP transcription factors with TOPLESS/TOPLESS-RELATED corepressors and modulates leaf development in *Arabidopsis*. *Plant Cell* **25**, 421–437 (2013).
30. Y. Yang, M. Nicolas, J. Zhang, H. Yu, D. Guo, R. Yuan, T. Zhang, J. Yang, P. Cubas, G. Qin, The TIE1 transcriptional repressor controls shoot branching by directly repressing BRANCHED1 in *Arabidopsis*. *PLOS Genet.* **14**, e1007296 (2018).
31. J. Zhang, B. Wei, R. Yuan, J. Wang, M. Ding, Z. Chen, H. Yu, G. Qin, The *Arabidopsis* RING-type E3 ligase TEAR1 controls leaf development by targeting the TIE1 transcriptional repressor for degradation. *Plant Cell* **29**, 243–259 (2017).
32. C. van den Berg, V. Willemsen, G. Hendriks, P. Weisbeek, B. Scheres, Short-range control of cell differentiation in the *Arabidopsis* root meristem. *Nature* **390**, 287–289 (1997).
33. Y. Zhang, Y. Jiao, Z. Liu, Y. X. Zhu, ROW1 maintains quiescent centre identity by confining *WOX5* expression to specific cells. *Nat. Commun.* **6**, 6003 (2015).
34. A. Heyl, E. Ramireddy, W. G. Brenner, M. Riefler, J. Allemeersch, T. Schmulling, The transcriptional repressor ARR1-SRDX suppresses pleiotropic cytokinin activities in *Arabidopsis*. *Plant Physiol.* **147**, 1380–1395 (2008).
35. A. Bhargava, I. Clabaugh; J. P. To, B. B. Maxwell, Y. H. Chiang, G. E. Schaller, A. Loraine, J. J. Kieber, Identification of cytokinin-responsive genes using microarray meta-analysis and RNA-Seq in *Arabidopsis*. *Plant Physiol.* **162**, 272–294 (2013).
36. T. L. Bailey, J. Johnson, C. E. Grant, W. S. Noble, The MEME Suite. *Nucleic Acids Res.* **43**, W39–W49 (2015).
37. L. Yuan, Z. Liu, X. Song, C. Johnson, X. Yu, V. Sundaresan, The CKI1 histidine kinase specifies the female gametic precursor of the endosperm. *Dev. Cell* **37**, 34–46 (2016).
38. R. Hehl, L. Bulow, AthaMap web tools for the analysis of transcriptional and posttranscriptional regulation of gene expression in *Arabidopsis thaliana*. *Methods Mol. Biol.* **1158**, 139–156 (2014).
39. A. J. Cary, W. Liu, S. H. Howell, Cytokinin action is coupled to ethylene in its effects on the inhibition of root and hypocotyl elongation in A*rabidopsis thaliana* seedlings. *Plant Physiol.* **107**, 1075–1082 (1995).
40. K. N. Chang, S. Zhong, M. T. Weirauch, G. Hon, M. Pelizzola, H. Li, S. S. Huang, R. J. Schmitz, M. A. Urich, D. Kuo, J. R. Nery, H. Qiao, A. Yang, A. Jamali, H. Chen, T. Ideker, B. Ren, Z. Bar-Joseph, T. R. Hughes, J. R. Ecker, Temporal transcriptional response to ethylene gas drives growth hormone cross-regulation in *Arabidopsis*. *eLife* **2**, e00675 (2013).
41. Y. Shi, S. Tian, L. Hou, X. Huang, X. Zhang, H. Guo, S. Yang, Ethylene signaling negatively regulates freezing tolerance by repressing expression of *CBF* and type-A *ARR* genes in *Arabidopsis*. *Plant Cell* **24**, 2578–2595 (2012).
42. J. A. Long, C. Ohno, Z. R. Smith, E. M. Meyerowitz, TOPLESS regulates apical embryonic fate in *Arabidopsis*. *Science* **312**, 1520–1523 (2006).
43. L. Wang, B. Wang, L. Jiang, X. Liu, X. Li, Z. Lu, X. Meng, Y. Wang, S. M. Smith, J. Li, Strigolactone signaling in *Arabidopsis* regulates shoot development by targeting D53-Like SMXL repressor proteins for ubiquitination and degradation. *Plant Cell* **27**, 3128–3142 (2015).
44. J. F. Palatnik, E. Allen, X. Wu, C. Schommer, R. Schwab, J. C. Carrington, D. Weigel, Control of leaf morphogenesis by microRNAs. *Nature* **425**, 257–263 (2003).
45. I. Hwang, J. Sheen, B. Muller, Cytokinin signaling networks. *Annu. Rev. Plant Biol.* **63**, 353–380 (2012).
46. B. Ren, Y. Liang, Y. Deng, Q. Chen, J. Zhang, X. Yang, J. Zuo, Genome-wide comparative analysis of type-A *Arabidopsis* response regulator genes by overexpression studies reveals their diverse roles and regulatory mechanisms in cytokinin signaling. *Cell Res.* **19**, 1178–1190 (2009).
47. B. Muller, J. Sheen, Cytokinin and auxin interaction in root stem-cell specification during early embryogenesis. *Nature* **453**, 1094–1097 (2008).
48. R. Di Mambro, M. De Ruvo, E. Pacifici, E. Salvi, R. Sozzani, P. N. Benfey, W. Busch, O. Novak, K. Ljung, L. Di Paola, A. F. M. Maree, P. Costantino, V. A. Grieneisen, S. Sabatini, Auxin minimum triggers the developmental switch from cell division to cell differentiation in the *Arabidopsis* root. *Proc. Natl. Acad. Sci. U.S.A.* **114**, E7641–E7649 (2017).
49. H. Takatsuka, T. Higaki, M. Umeda, Actin reorganization triggers rapid cell elongation in roots. *Plant Physiol.* **178**, 1130–1141 (2018).
50. J. P. Vogel, K. E. Woeste, A. Theologis, J. J. Kieber, Recessive and dominant mutations in the ethylene biosynthetic gene *ACS5* of *Arabidopsis* confer cytokinin insensitivity and ethylene overproduction, respectively. *Proc. Natl. Acad. Sci. U.S.A.* **95**, 4766–4771 (1998).
51. T. I. Baskin, A. Cork, R. E. Williamson, J. R. Gorst, *STUNTED PLANT 1*, a gene required for expansion in rapidly elongating but not in dividing cells and mediating root growth responses to applied cytokinin. *Plant Physiol.* **107**, 233–243 (1995).
52. A. Kuderova, I. Urbankova, M. Valkova, J. Malbeck, B. Brzobohaty, D. Nemethova, J. Hejatko, Effects of conditional IPT-dependent cytokinin overproduction on root architecture of *Arabidopsis* seedlings. *Plant Cell Physiol.* **49**, 570–582 (2008).
53. M. G. Mason, D. E. Mathews, D. A. Argyros, B. B. Maxwell, J. J. Kieber, J. M. Alonso, J. R. Ecker, G. E. Schaller, Multiple type-B response regulators mediate cytokinin signal transduction in *Arabidopsis*. *Plant Cell* **17**, 3007–3018 (2005).
54. I. H. Street, D. E. Mathews, M. V. Yamburkenko, A. Sorooshzadeh, R. T. John, R. Swarup, M. J. Bennett, J. J. Kieber, G. E. Schaller, Cytokinin acts through the auxin influx carrier AUX1 to regulate cell elongation in the root. *Development* **143**, 3982–3993 (2016).
55. W. Zhou, L. Wei, J. Xu, Q. Zhai, H. Jiang, R. Chen, Q. Chen, J. Sun, J. Chu, L. Zhu, C. M. Liu, C. Li, *Arabidopsis* Tyrosylprotein sulfotransferase acts in the auxin/PLETHORA pathway in regulating postembryonic maintenance of the root stem cell niche. *Plant Cell* **22**, 3692–3709 (2010).
56. E. Salvi, R. Di Mambro, S. Sabatini, Dissecting mechanisms in root growth from the transition zone perspective. *J. Exp. Bot.* **71**, 2390–2396 (2020).
57. J. Miao, D. Guo, J. Zhang, Q. Huang, G. Qin, X. Zhang, J. Wan, H. Gu, L. Qu, Targeted mutagenesis in rice using CRISPR-Cas system. *Cell Res.* **23**, 1233–1236 (2013).
58. Z.-P. Wang, H.-L. Xing, L. Dong, H.-Y. Zhang, C.-Y. Han, X.-C. Wang, Q.-J. Chen, Egg cell-specific promoter-controlled CRISPR/Cas9 efficiently generates homozygous mutants for multiple target genes in *Arabidopsis* in a single generation. *Genome Biol.* **16**, 144 (2015).
59. J. Lan, J. Zhang, R. Yuan, H. Yu, F. An, L. Sun, H. Chen, Y. Zhou, W. Qian, H. He, G. Qin, TCP transcription factors suppress cotyledon trichomes by impeding a cell differentiation-regulating complex. *Plant Physiol.* **186**, 434–451 (2021).
60. X. Zheng, J. Lan, H. Yu, J. Zhang, Y. Zhang, Y. Qin, X. D. Su, G. Qin, *Arabidopsis* transcription factor TCP4 represses chlorophyll biosynthesis to prevent petal greening. *Plant Commun.* **3**, 100309 (2022).

Acknowledgments: We thank L.-J. Qu (Peking University) and H. Gu (Peking University) for support and suggestions. We thank Y. Zhu (Peking University) for providing the seeds of QC marker WOX5::GFP, L. Yuan (Northwest Agriculture & Forestry University) for the seeds of the TCSn::NLS-3×GFP marker, Y. Hu (Institute of Botany, Chinese Academy of Sciences) for the seeds of CyclinB1;1:GUS, and S. Yang (China Agricultural University) for the seeds of *arr1* and *arr2*. We also thank the Core Facilities of Life Sciences, Peking University, the National Center for Protein Sciences at Peking University, and L. Fu for assistance with confocal microscopy. **Funding:** This research was supported by the National Science Fund for Distinguished Young Scholars of China (grant no. 31725005) and the Science Fund for the Creative Research Groups of the National Natural Science Foundation of China (grant no. 31621001). **Author contributions:** G.Q. supervised and designed the study. Q.H. and R.Y. performed most of the experiments. T.Z. generated the genetic materials and performed some of the experiments. F.A., N.W., J.L., X.W., Z.Z., Y.P., and X.W. performed some of the experiments and/or analyzed the data. D.G. and J.Z. generated the genetic materials. G.Q., Q.H., and R.Y. analyzed the results. G.Q., Q.H., and R.Y. wrote the manuscript. **Competing interests:** The authors declare that they have no competing interests. **Data and materials availability:** All data needed to evaluate the conclusions in the paper are present in the paper and/or the Supplementary Materials.

Submitted 1 December 2021
Accepted 25 July 2022
Published 9 September 2022
10.1126/sciadv.abn5057